

AD-A016 612

EXPERIMENTAL APPLICATIONS OF THE MODULAR ACOUSTIC SYSTEM
FOR THE SUBMERSIBLE ALVIN

Paul T. McElroy

Bolt Beranek and Newman, Incorporated

Prepared for:

Office of Naval Research

August 1975

DISTRIBUTED BY:



National Technical Information Service
U. S. DEPARTMENT OF COMMERCE

311081

BOLT BERANEK AND NEWMAN INC

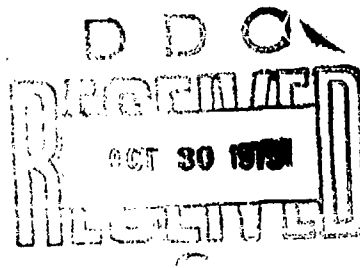
CONSULTING · DEVELOPMENT · RESEARCH

ADA016612 Report No. 3110

EXPERIMENTAL APPLICATIONS OF THE MODULAR ACOUSTIC
SYSTEM FOR THE SUBMERSIBLE ALVIN

P.T. McElroy

August 1975



Research sponsored by the Office of Naval Research under
Contract No. N00014-75-C-0659; NR260-113.
Reproduction in whole or in part is permitted for any
purpose of the United States Government.

Reproduced by
NATIONAL TECHNICAL
INFORMATION SERVICE
U.S. Department of Commerce
Springfield, VA 22151

DISTRIBUTION STATEMENT A
Approved for public release;
Distribution Unlimited

CAMBRIDGE WASHINGTON, D.C. CHICAGO HOUSTON LOS ANGELES SAN FRANCISCO

Unclassified

SECURITY CLASSIFICATION OF THIS PAGE (When Data Entered)

DD FORM 1473 EDITION OF 1 NOV 65 IS OBSOLETE
1 JAN 73

Unclassified

SECURITY CLASSIFICATION OF THIS PAGE (When Data Entered)

Unclassified

SECURITY CLASSIFICATION OF THIS PAGE (When Data Entered)

19. Key Words (Cont.)

Slope Water
Scattering Cross Section
Microtopography
Bottom Scattering

Sampling of Bottom Topography
Near-Bottom
Seismic Profiling at 3.5 kHz

20. Abstract (Cont.)

angle of incidence, with particular attention to the porosity created in marine sediments by large populations of marine tube-building organisms, including polychaete worms and pogonophorans.

2. Scattering, as a function of frequency, from fish of the deep scattering layer in those special cases where only one species and one size of fish is present.

3. Measurement of the small-scale topography of the ocean bottom, and relation of that topography to scattering of energy measured as a function of frequency and angle.

4. Near-bottom seismic profiling at 3.5 kHz and higher frequencies.

In each case, attention is given to relevant theory, description of the environmental factors including possible sites, instrumentation needed in addition to the Modular Acoustic System, and discussion of other measurements that should be made to provide better correlation of acoustic results with the environmental factors.

1a Unclassified
SECURITY CLASSIFICATION OF THIS PAGE (When Data Entered)

Report No. 3110

EXPERIMENTAL APPLICATIONS OF THE MODULAR ACOUSTIC
SYSTEM FOR THE SUBMERSIBLE ALVIN

P.T. McElroy

August 1975

Research sponsored by the Office of Naval Research under
Contract No. N00014-75-C-0659; NR260-113.
Reproduction in whole or in part is permitted for any
purpose of the United States Government.

Prepared by:

Bolt Beranek and Newman Inc.
50 Moulton Street
Cambridge, Massachusetts 02138

ABSTRACT

The Modular Acoustic System is a broadband general purpose acoustic measurement system designed for use on the submersible ALVIN. This report discusses four general areas for experimental research where the design features of the System, coupled with ALVIN's special capabilities, are particularly appropriate. The areas are:

1. Bottom reflectivity as a function of both frequency and angle of incidence, with particular attention to the porosity created in marine sediments by large populations of marine tube-building organisms, including polychaete worms and pogonophorans.
2. Scattering, as a function of frequency, from fish of the deep scattering layer in those special cases where only one species and one size of fish is present.
3. Measurement of the small-scale topography of the ocean bottom, and relation of that topography to scattering of energy measured as a function of frequency and angle.
4. Near-bottom seismic profiling at 3.5 kHz and higher frequencies.

In each case, attention is given to relevant theory, description of the environmental factors including possible sites, instrumentation needed in addition to the Modular Acoustic System, and discussion of other measurements that should be made to provide better correlation of acoustic results with the environmental factors.

TABLE OF CONTENTS

	page
ABSTRACT	iii
LIST OF FIGURES AND TABLES	ix
SECTION 1. INTRODUCTION	1
REFERENCES, SEC. 1	4
2. BOTTOM REFLECTIVITY WITH SPECIAL ATTENTION TO THE EFFECTS OF TUBE-BUILDING MARINE ORGANISMS	5
2.1 Introductory Comments	5
2.2 The Porous Features of Sediments	9
2.3 Living Organisms and Marine Sediment Porosity	11
2.4 Dispersive Characteristics of Porous Media	14
2.5 Spectral Measurements of Reflectivity ..	18
2.6 Reflectivity at Oblique Incidence	20
2.7 Spherical Wave Modifications to the Plane Wave Approximation	23
2.8 The Layer Thickness Created by Tube- Building Marine Organisms	26
2.9 Determination of the Reflection Coefficient	27
2.10 The Mechanical Properties of Sediments.	28
2.11 Experimental Sites	29
2.12 Supplemental Instrumentation	32
2.13 Conclusions	34
REFERENCES, SEC. 2	35

Preceding page blank

TABLE OF CONTENTS (Cont.)

	page
SECTION 3. SPECTRAL MEASUREMENTS OF GROUPS OF A SINGLE SPECIES OF FISH	39
3.1 Introduction	39
3.2 Theoretical Background	40
3.2.1 Bladder equations for a single fish	40
3.2.2 Group effects	42
3.2.3 Depth dependence	44
3.2.4 Multiple scattering	45
3.3 Experimental Background	49
3.4 Application of the Modular Acoustic System to Spectral Measurements of the Deep Scattering Layer	50
3.5 Experimental Sites	52
3.6 Fish Identification and Sampling	56
3.7 Conclusions	58
REFERENCES, SEC. 3	59
4. MICROTOPOGRAPHY AND SCATTERING	63
4.1 Introductory Comments	63
4.2 Theoretical Background - Scattering ..	63
4.3 Determination of Microtopography from ALVIN	68
4.3.1 Deterministic measurement of $\xi(\vec{r}_A)$	68
4.3.2 Statistical measurement of $\xi(r_A)$	70
4.4 Scattering Measurements	77
4.5 Supplemental Instrumentation	78
4.6 Experimental Sites	80
4.7 Conclusions	80
REFERENCES, SEC. 4	82

TABLE OF CONTENTS (Cont.)

	page
SECTION 5. SEISMIC PROFILING AT 3.5 kHz	83
5.1 Background Discussion	83
5.2 Penetration into the Bottom	85
5.3 Supplemental Instrumentation.....	90
5.3.1 ALNAV	90
5.3.2 Precision depth indicator	94
5.3.3 Precision time base	94
5.3.4 Cores	95
5.4 Conclusions	95
REFERENCES, SEC. 5	97

LIST OF FIGURES AND TABLES

	page
Figure 2.1 Geometry for reflectivity measurements	7
2.2 Reflection coefficient vs frequency for a fluid in a rigid solid matrix	19
4.1 Geometry for statistical sampling of the height of the deviations of the area A_0 from flatness, $\xi(\vec{r}_A)$	72
4.2 Probability of sampling an area A at a distance r_A from the center (relative to the radius of the sampled area, r_0), normalized by the probability of sampling at the center ($r_A=0$). ..	76
Table 2.1 Characteristic frequency of tubes	15
5.1 Comparison of three 3.5/4-kHz systems and one system at 6 kHz for bottom penetration ..	86

Preceding page blank

1. INTRODUCTION

In this report, we describe several experiments that could be made with the Modular Acoustic System, now nearing completion, while it is mounted on the deep submergence research vehicle ALVIN.

Development of the Modular Acoustic System began in late 1972. It is a part of the instrument development program for ALVIN that the Advanced Research Projects Agency of the Department of Defense started funding in 1970. The vehicle itself had been designed, built, and operated with Office of Naval Research funds from 16 June 1961 to 31 December 1973. Experiments conducted on ALVIN during that period have been summarized in the Woods Hole Oceanographic Institution technical report WHOI-74-60 (1974). ONR support culminated in the installation of a titanium sphere that increased the depth capability of ALVIN to 12,000 ft.

The ARPA contract has funded a series of instruments, all designed to enhance ALVIN's measurement capabilities and, simultaneously, to employ high-level, high-risk technology. The Modular Acoustic System is one of the series; the first tests of this acoustic instrumentation system on ALVIN in May 1975 disclosed some residual problems expected to be resolved by December 1975.

Features of the system are discussed fully in the original proposal to ARPA (McElroy and Hess, 1972) and in McElroy (1975). Briefly, the system is composed of an external transducer mount that is trainable in azimuth and elevation and of three interchangeable transducers, detuned to cover the frequency range from 2 to 45 kHz. Extensive operator control over parameters such as transducer position, operating frequency and pulse length, and spectral scanning is possible with either a manual control system

or a more complicated computerized system. Data loggers, analog tape recorders, and the computer record various operating parameters and experimental acoustic returns. A visual display is available for use during a dive to permit optimization of experimental conditions; for instance, the frequency spacing in spectral measurements can be adjusted, based on the appearance of a measured spectrum.

When the Modular Acoustic System is mounted on ALVIN, the experimenter can acoustically sample a much smaller surface or volume than is possible with transducer systems operating at the surface. Data comparisons can be made with results from other on-site instrumental packages, such as rock hammers and drills, and plankton nets, already developed for use on ALVIN.

We believe that the addition of the Modular Acoustic System will enhance the uniqueness of ALVIN, displayed most recently in studies of the mid-Atlantic ridge during Project FAMOUS. During that project, observers trained in the geological and geophysical sciences recorded details of the immediate environs of the rift valley (Ballard, 1975; Heirtzler, 1975; Heirtzler and Bryan, 1975; Hammond, 1975).

ALVIN's ability to come close to areas of interest in the deep sea, demonstrated clearly during Project FAMOUS, would be combined with the Modular Acoustic System, in the experiments suggested in this report, to provide information not easily attainable by other means.

In planning these experiments, we have attempted to answer the following questions:

- What is the scientific or technical question to be answered?

- What is the relevant mathematical formalism, provided it exists?
- How might the experiment be carried out, giving attention to the geographic area and season of the year, if appropriate, and to those portions of the system necessary for the experiment? Instrumental features that do not exist, but which might be added, are considered.
- What other measurements could be made nearly simultaneously that could enhance the relevance or interpretability of the acoustic results?

The experimental problems specifically addressed in this report are:

- Studies of bottom reflectivity in the presence of tube-building marine organisms (Sec. 2).
- Volume reverberation, particularly in areas where a single species is present (Sec. 3).
- Bottom topography descriptions, both for geomorphological purposes and as a means of determining the bottom parameters relevant to scattering experiments (Sec. 4).
- Near-bottom seismic profiling at 3.5 kHz (Sec. 5).

REFERENCES, SEC. 1

Ballard, R.D. (1975). "Dive into the Great Rift," *National Geographic* 147:604-615.

Hammond, A.L. (1975). "Project FAMOUS: Exploring the Mid-Atlantic Ridge," and "Submersibles: A Research Technology whose Time has Come?" *Science* 187:823-825.

Heirtzler, J.R. (1975). "Where the Earth Turns Inside Out," *National Geographic* 147:586-603.

Heirtzler, J.R. and W.B. Bryan (1975). "The Floor of the Mid-Atlantic Rift," *Sci. Am.* 233:78-90.

McElroy, P.T. and F.R. Hess (1972). "A Deep Submersible Modular Acoustic System," appearing in *Advanced Marine Technology*, a Research Proposal submitted to the Advanced Research Projects Agency of the Department of Defense by the Woods Hole Oceanographic Institution, Woods Hole, Mass., Sept. 30, 1972. Dr. Robert W. Morse, Principal Investigator.

McElroy, P.T. (1975). "Design Features of the Submersible Modular Acoustic System," BBN Report No. 3060 (Bolt Beranek and Newman Inc., Cambridge, Mass.)

Woods Hole Oceanographic Institution (1974). "Deep Submergence Research Conducted During the Period 16 June 1961 through 31 December 1973," Technical Report WHOI-74-60.

2. BOTTOM REFLECTIVITY WITH SPECIAL ATTENTION TO THE EFFECTS OF TUBE-BUILDING MARINE ORGANISMS

2.1 Introductory Comments

In this section, we discuss acoustic studies of ocean bottoms lying within the 12,000-ft depth range of ALVIN. In many regions, the bottom is composed of sediments that are porous. The porosity arises either from the very small interstitial spaces between sedimentary grains or from a new source we consider: the network of tubes created by certain marine organisms. We emphasize this latter cause and examine the polychaete worm *Hyalinoecia* and the pogonophorans as specific examples. Reflectivity as a function of both frequency and angle is considered when the sediments have been modified by these tube-builders. We discuss possible sites for experiments in general terms because of the limited data on densities of benthic fauna.

The reflection coefficient of sound incident on a surface is a function of the sound velocities, densities, and attenuation in the two media separated by the surface as well as a function of the angle of incidence (Morse and Ingard, 1968). A series of plots for this coefficient vs angle for a number of possible conditions at the interface of ocean and sedimentary bottoms is found in MacKenzie (1960); the modifications to the reflectivity due to attenuation in the bottom are illustrated.

If the attenuation and sound velocity in ocean bottom sediments are frequency dependent, then the reflection coefficient will in general be a function of frequency, as the following over simplified equation shows (Eq. 2.1). It is the reflection coefficient at a liquid-liquid interface, such as would be appropriate

if the bottom could not support transverse waves (Brekhovskikh, 1960, Eqs. 3.16, 3.17, 3.10).

$|V|$ = Reflection coefficient

$$= \frac{\rho_2 c_2}{\cos\theta_2} - \frac{\rho_1 c_1}{\cos\theta_1} \quad (2.1)$$

$$= \frac{\rho_2 c_2}{\cos\theta_2} + \frac{\rho_1 c_1}{\cos\theta_1}$$

$$\cos\theta_2 = \left[1 - \left(\frac{c_2}{c_1} \right)^2 \sin^2\theta_1 \right]^{1/2} \quad (2.2)$$

where index 1 applies to the upper medium (sea water) and index 2 applies to the lower (sediment) (Fig. 2.1). The c 's are the sound velocities in the two media and the ρ 's are the densities; c_2 and θ_2 can be complex; a complex c_2 occurs for a lossy medium, while complex θ_2 occurs for both a complex c_2 and angles θ_1 in excess of the critical angle.

The velocity c_2 occurs in the expression for a plane wave in the form

$$e^{-ik_2 z \cos\theta_2} = e^{-\frac{i\omega}{c_2} z \cos\theta_2}$$

for propagation in the $-z$ direction. If the phase velocity in medium two is represented by v_2 and the attenuation per unit distance by α_2 , then k_2 can be reexpressed as (MacKenzie, 1960)

$$k_2 = \omega/v_2 + i\alpha_2 \quad (2.3)$$

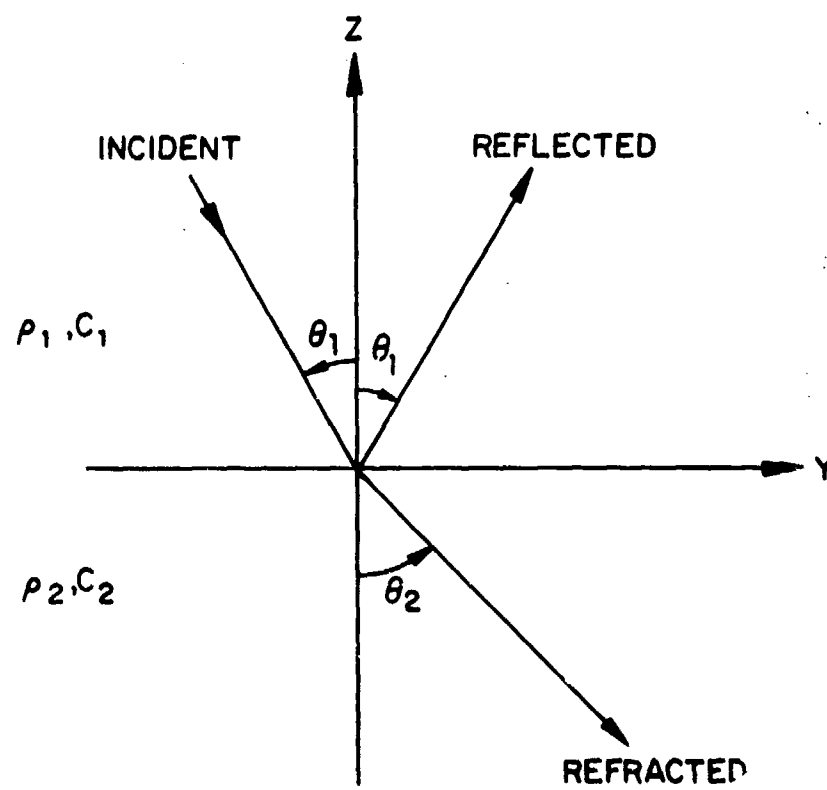


FIG. 2.1. GEOMETRY FOR REFLECTIVITY MEASUREMENTS.

Solving for c_2 gives

$$c_2 = v_2 \times \left[1 + \left(\frac{\alpha_2}{\omega} v_2 \right)^2 \right]^{-1} - i \frac{\alpha_2}{\omega} v_2^2 \times \left[1 + \left(\frac{\alpha_2}{\omega} v_2 \right)^2 \right]^{-1}. \quad (2.4)$$

This expression for c_2 permits evaluation of the reflection coefficient (Eq. 2.1) both for arbitrary phase velocity and attenuation in the lower medium.

However, this form of c_2 proves to be unduly complicated for ocean sediments, since $(\alpha_2/\omega)v_2$ is much less than 1. When attenuation values from Fig. 1 of Hamilton (1974) are used, $(\alpha_2/\omega)v_2$ is less than 0.003, and c_2 simplifies to

$$c_2 = v_2 - i(\alpha_2/\omega) v_2^2. \quad (2.5)$$

Extensive measurements of phase velocity and attenuation have been reported in the literature and summarized by Hamilton (1974). With firmness, he concludes that the phase velocity is nondispersing, and that α_2 shows dependence on the first power of frequency. The immediate implication from Eqs. 2.4 and 2.5 is that c_2 , and hence the reflection coefficient, are independent of frequency.

This fact has an immediate bearing on the applicability of the Modular Acoustic System to measurements of the spectral properties of bottom sediments; to the degree to which Hamilton's assessment is true, spectral measurements of reflectivity would be unproductive. However, a series of experiments to confirm Hamilton's position would be useful, particularly in view of the scatter in the data on which Hamilton bases his judgment. Of even greater interest would be a series of spectral measurements on bottom

sediments that deviate significantly from usual laboratory conditions or from the conditions encountered in many at-sea experiments. The highly porous sediments that result from the burrowing activities of large populations of living organisms, such as marine worms, could provide the basis for these experiments.

2.2 The Porous Features of Sediments

Investigators have been concerned with very small-scale porosity in sediments arising from the intermixture of water and the individual particles of the sedimentary material. The resultant sediments vary from those that are in large measure water to those partially-consolidated sediments that have little pore water.

The most extensive theoretical investigations are those of Biot (1956a,b; 1962a,b), recently reexamined by Stoll (1974). The resulting model includes motion of the fluid relative to the viscoelastic frame, resulting in (1) an effective density for the water up to three times the normal density, and (2) viscous loss in the fluid due to boundary layer flow. Later refinements added the viscous effects of solid grains rubbing against one another. The net result is a theoretical prediction of α vs frequency showing a 2nd-power dependence at low frequencies and a 1/2-power dependence at high frequencies for high-permeability sediments such as sands and turbidites (Stoll, Figs. 2 and 3, 1974).* The pore sizes assumed in Stoll's calculations were 10^{-2} to 10^{-4} cm. Phase and group velocities are also predicted by this theory.

*These power laws are modified when viscous effects in the solid are included.

The formalism is elegant and has been profitably applied to the interaction of air with porous materials (Morse and Ingard, 1968; Galaitsis and Ingard, 1974; Noiseux *et al.*, 1975). Yet it is this viscoelastic model for ocean sediments that Hamilton (1974) dismisses when he reviews actual measurements of v_2 and α_2 . Apparently, the fluid does not move relative to the frame, and thus losses from this source do not occur.

There is another type of porosity that has not been examined, however. This porosity is the result of the presence of tubular structures in the surficial layers of the sediments, created by marine organisms such as polychaetes and pogonophorans. These tubes penetrate the surface and are often of much larger diameter than the pores considered by Stoll. Thus, it is quite possible that there could be significant motion of the fluid relative to the frame and, hence, loss. As the densities of the numbers of these animals can be high (creating sediments said to look like Swiss cheese), the effect of numerous tubes could be significant.

Biot's (1956a,b) theoretical analysis has direct applicability, since one of the pore types he considers is a cylindrical tube. We will see below that the frequency dependence of viscous losses in a tube is dependent on its diameter; the smaller the diameter, the higher the frequency at which peaks in the loss per cycle occur. Thus, the tubes that are smaller in diameter and shallower will be associated with structure in attenuation and dispersion at higher frequencies. The diameter of these tubes is much larger than that of the pores normally found in unconsolidated sediments, and, hence, may show the dispersive effects not seen in normal sediments.

2.3 Living Organisms and Marine Sediment Porosity

Sedimentary infauna, including tube-building species, have been studied extensively in shallow water environments, where many investigators have devoted their professional careers to the taxonomic description of the fauna and more recently to important factors affecting faunal distribution into communities and the resultant flow of energy (Rhoads and Young, 1970; Aller and Dodge, 1974). The same questions have been examined in the deep sea (Rowe, 1971/1972; Grassle *et al.*, 1975), although far less is known there. A recent review (Rowe, 1974) contains a number of relevant comments. For instance, Rowe notes that the predicted great decrease in standing stock and in the rates of life processes in the deep sea are violated in a number of areas where activity is great. In this respect, we consider two types of deep-sea creatures: polychaetes and pogonophorans. Though each type is different in its evolution and behavior, each lives in a tube, and each has representative species that are known to be in population densities high enough to create porous sediments. For instance, Fauchald (1975) notes that a polychaete, *Hyalinoecia*, can have immense densities, perhaps attributable to its feeding pattern, since it is a scavenger of large carcasses.

Ivanov (1963), who has studied pogonophorans in great detail, writes that they "are numbered amongst the rather common animals of the oceans. They are found in nearly all seas." Some idea of the density of these unusual animals is given by the experience of scientists on the British ship, R.R.S. DISCOVERY II, who, while sampling the ocean bottom, discarded many tons of a matlike material facetiously called gubbinidae. Careful consideration after the fact showed the gubbins to be pogonophorans and their tubes (Carlisle, 1963).

Overall, the density of the ocean bottom infauna is highly variable; *Hyalinoecia* populations range from very small to immense (Fauchald, 1975). Fortunately, investigators have some idea of the effects of these populations on sediments. The shapes of excavations for shallow water species have been described and classified (Seilacher, 1964), and the effects on the mechanical properties of the sediments observed (Rhoads and Young, 1970; Fager, 1964). *Hyalinoecia* and the pogonophorans with their persistent tubes probably strengthen the sediment, while others weaken it by their sediment-overturning actions (Rowe, 1974). Table 1 in Rowe is a ready summary of these effects. However, even those worms that strengthen the sediments induce considerable variance in the geotechnical parameters (A. Richards, cited in Rowe, 1974).

The persistence of tubes can be variable. The tubes of some species decay within weeks of being abandoned (Fager, 1964), while the tubes of *Hyalinoecia* can last 20 or 30 years (Fauchald, 1975). High persistence of tubes, provided they do not fill with silt, implies a far greater effect on the porosity of the sediments than one might predict on the basis of the actual population of worms at any given time. Tubes in shallow water may be destroyed by predators which might not be active in the deep sea [e.g., the rays mentioned in Fager (1964)]. Pogonophoran tubes are made of a cellulose (Hyman, 1959). The persistence of this material, which has the consistency of soft leather, would depend on the biological activity of the surroundings.

The depth of tubes is another important variable in predicting acoustic effects. Many of these tube-builders are of great length compared to their diameter. The depths of their tubes are usually

limited to a small multiple of body length. This implies only a few centimeters for smaller species to meters for huge, but probably rare, individuals. Bezrukov and Romankovic (1960) cite deep-sea worms with tubes up to 4 m long. *Hyalinoecia* tubes are up to 30 cm long. Fauchald (1975) states that they are buried in the sediment. A contrary view is found in the photographs of Wigley and Emery (1967), where the tubes are shown lying on the bottom. However, these may be areas where *Hyalinoecia* has scavenged; Fauchald (1975) has observed *Hyalinoecia* dragging their tubes toward a newly-placed carcass.

Pogonophorans have a higher tube length-to-diameter ratio. The smallest species, *Siboglinum minutum*, has a tube 0.1 mm in diameter and up to 15 cm long (Ivanov, 1963). The largest species is *Zenkevitchiana longissima*, which has tubes 150 cm long (Ivanov, 1963).

Tube depth in some instances may exceed these figures. If turbidity currents with a high sediment load bury a region suddenly, there may be sequential layers of tubes with only the top-most layer containing living organisms.

Although we have concentrated on tube-building organisms, we should mention the other types which can be important in modifying sediments. There are numerous species, known as deposit feeders, which ingest sediments. Some of these vertically grade the sediments they ingest (Rhoads and Stanley, 1965) and may modify the sediment granularity for short periods through their feces (Rhoads, 1963).

The changes in granularity and addition of pore water by the action of the deposit feeders will change the sediment impedance

by changes in both density and sound velocity. These changes will result in changes in the reflectivity coefficient from area to area. In a given area, however, there is some question whether there will be any variation with frequency in the reflectivity, for the changes created by the deposit feeders are just changes in the porosity due to sediment grain size, and it is this porosity which Hamilton has claimed is not dispersive, as we have discussed above.

The tube builders and the deposit feeders comprise a large portion of the deep-sea infauna, or those animals that live in the sediment. Others, known as the epifauna, live on or just above the surface. The importance of epifauna lies more in modifications they make in the surface shape itself, and, hence, in the scattering of acoustic energy at wavelengths comparable to the size of these disturbances. For instance, the lobster *Homarus americanus* (Rowe, 1974) and the crab *Geryon quinquedens* (Grassle *et al.*, 1975) create large craters in sediments, and at 1800-m depths on the Gay Head-Bermuda transect many species contribute to small-scale relief in the bottom (Grassle *et al.*, 1975).

2.4 Dispersive Characteristics of Porous Media

Biot's theoretical studies on porous media (1956a,b, 1962a, b) provide a basis for determining the dependence of phase and group velocities and of attenuation on frequency. Central to this determination is the characteristic frequency f_c , that frequency at which viscous force caused by boundary layer flow of the fluid over the surface of the pores is comparable to the inertial force associated with the acceleration of the fluid mass within the pore. Biot has evaluated f_c for motion through sinuous tubes (1956b,

Eqs. 4.26 and 4.34), the very problem we are considering:

$$f_c = \frac{8}{3\pi} \frac{v\xi}{a^2} , \quad (2.6)$$

where a is the tube radius, v is the kinematic viscosity of the fluid, and ξ is a factor introduced *ad hoc* to account for sinuosity. Biot assumes ξ lies in or near the range of 1 to 1.5.

For water at 0°C, $v = 1.792 \times 10^{-2}$ (Condon and Odishaw, 1967). Setting $\xi = 1.5$, we get for f_c :

TABLE 2.1. CHARACTERISTIC FREQUENCY OF TUBES

a in cm	10^{-3}	3×10^{-3}	5×10^{-3}	10^{-2}	10^{-1}	1
f_c in Hz	23,000	2500	910	230	2.3	0.023

We will examine the significance of f_c after discussing the waves generated in the porous medium. Three waves are possible (two longitudinal and one transverse*) that involve coupled motions of the fluid and the supporting solid matrix, i.e., the sediment. The longitudinal wave of the first kind (using Biot's terminology) is the faster of the two longitudinal waves and is one where fluid motion and matrix motion are in phase. For certain relative values of some of the density and elastic parameters of the solid-fluid system, these two motions are of the same amplitude, and viscous attenuation in the fluid goes to zero. This condition, known as dynamic compatibility, seems unlikely to occur very often. In the longitudinal wave of the second kind, the velocity is slower,

*Biot calls the longitudinal waves dilatational and the transverse waves, rotational.

and the motions of fluid and solid are opposite in phase, resulting in much larger fluid viscous losses.

Thus, a plane wave incident on the medium from the water can excite three rather than the usual two waves in the solid medium. We will examine the experimental consequences of this in the subsection on reflectivity at oblique incidence.

The characteristic frequency f_c is a convenient frequency with which to describe the shapes of the velocity and attenuation curves. For instance, attenuation per cycle of transverse waves and longitudinal waves of the first kind peak at frequencies between one and two times the characteristic frequency. Phase and group velocities of all three waves become nondispersive at very high frequencies relative to f_c . f_c or some small integral multiple of it is the frequency at which phase and group velocity curves vs frequency show a knee separating the low-frequency regions where they are sharply dispersive and the intermediate frequency regions where they are more slowly dispersive.

For frequencies many times f_c , the attenuation α of all three waves becomes proportional to $f^{\frac{1}{2}}$, while the phase velocity becomes independent of frequency. Examination of Eqs. 2.4 and 2.5 shows that the complex sound velocity c_2 is then dependent on frequency (to the $-1/2$ power) and hence the reflection coefficient will be frequency dependent. Some features of the dependence can be inferred from Eq. 2.1 for $|V|$, although it is correct only for one longitudinal wave in the sedimentary medium and not for the three waves that actually occur. For instance if we represent $\alpha_2 = kf^{-\frac{1}{2}}$, use Eq. 2.5 for c_2 , and set $\theta_1 = 0$ for normal incidence, then

$$|V| = \left[\frac{(\rho_2 v_2 - \rho_1 c_1)^2 + k^2 f^{-1} \rho_2^2}{(\rho_2 v_2 + \rho_1 c_1)^2 + k^2 f^{-1} \rho_2^2} \right]^{\frac{1}{2}} \quad (2.7)$$

This expression asymptotically approaches

$$\frac{(\rho_2 v_2 - \rho_1 c_1)}{(\rho_2 v_2 + \rho_1 c_1)}$$

from above as frequency is increased.

Determination of the reflection coefficient for porous media requires matching the boundary conditions simultaneously for the three waves. That calculation has not been carried out, although this would need to be done prior to any successful comparison of acoustic measurements with sediment properties. The reflection coefficient vs frequency has been computed for the much simpler situation in which the sediment matrix is considered rigid, so that only one wave, the fluid longitudinal wave, is created. Equation 6.3.16 from Morse and Ingard (1968) is used for the reflection coefficient

$$V = \frac{\rho_p c_p (\omega + i\Phi/\rho_p) \cos \theta_1 - \rho_1 c_1 (\omega^2 \cos^2 \theta_2 + i\omega\Phi/\rho_p)^{\frac{1}{2}}}{\rho_p c_p (\omega + i\Phi/\rho_p) \cos \theta_1 + \rho_1 c_1 (\omega^2 \cos^2 \theta_2 + i\omega\Phi/\rho_p)^{\frac{1}{2}}} \quad (2.8)$$

where ρ_p is the effective density of the fluid in the pores and is some small multiple of the actual density ρ_2 ; $c_p^2 = 1/\rho_p \kappa_p \Omega$, the wave velocity; κ_p is the effective compressibility of the fluid; Ω is the porosity of the sediment (fraction occupied by water); Φ is the viscous loss parameter, proportional to the absolute viscosity; and θ_2 , the refracted angle, is given by

$$\cos^2 \theta_2 = 1 - (c_p/c_1)^2 \sin^2 \theta_1.$$

The calculation is plotted in Fig. 2.2 for values of ρ_p and ϕ chosen to bring the structure in reflectivity within the frequency range of the Modular Acoustic System. It can be seen that the variation with frequency is strong and that the structure is dependent on the angle of incidence.

The conclusion is that reflectivity will show a small dependence on frequency for frequency ranges well above the characteristic frequency and will show sharper structure for ranges spanning the characteristic frequency.

2.5 Spectral Measurements of Reflectivity

What we might hope to see in a spectral measurement of ocean sediments is dependent on where f_c lies in relation to the frequency range of the Modular Acoustic System (2 to 45 kHz) for tubes of living organisms. We will discuss the sites of possible experiments in more detail in Sec. 2.11. For the moment, let us consider three sizes of tubes. Rowe (1975) has been investigating a region with a high density of abandoned tubes that are about 1 cm in diameter. *Hyalinoecia* tubes are about 0.3 cm in diameter, while the smallest pogonophoran tubes are 0.1 mm in diameter. The characteristic frequency for the first two (Table 2.1) is well below the lowest frequency of the acoustic system, and so a spectral measurement of reflectivity would show only slowly varying structure with frequency or perhaps no structure if the asymptotic value had been reached. However, f_c for the small pogonophoran tube is about 1000 Hz, so that strong structure could be expected to lie within the frequency range of the system. Measurement of that structure could in turn be related to the parameters describing the porous system, namely the density (ρ_{11} , ρ_{12} , ρ_{22})

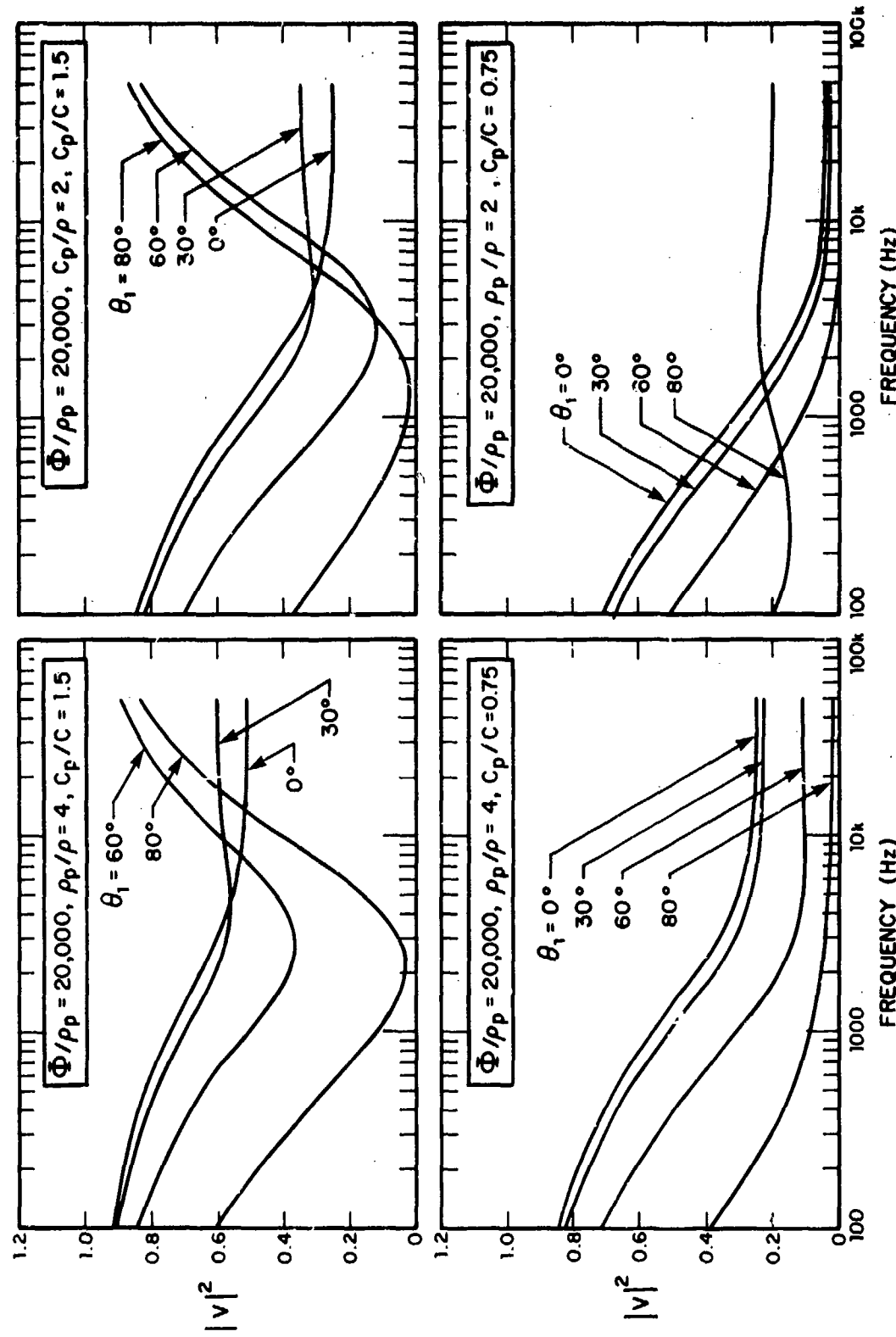


FIG. 2.2. REFLECTION COEFFICIENT VS FREQUENCY FOR A FLUID IN A RIGID SOLID MATRIX. IN EACH GRAPH, THE FOUR CURVES CORRESPOND TO THE INCIDENT ANGLE, θ_1 , EQUAL TO 0° , 30° , 60° , and 80° . THE FOUR INDIVIDUAL GRAPHS CORRESPOND TO DIFFERENT VALUES OF EFFECTIVE MASS, ρ_p , AND WAVE VELOCITY c_p .

and elasticity parameters (P, Q, R) (Biot, 1956a), which are both relatable to the porosity (Ω) of the solid-fluid system. Reflectivity measurements conducted at normal incidence would aid in determining these parameters, which could be supplemented profitably by measurements at oblique incidence. The elasticity parameters can be determined independently in static tests (Stoll, 1974).

2.6 Reflectivity at Oblique Incidence

Since the Modular Acoustic System uses the same transducer as source and receiver, it measures backscatter rather than reflectivity, except at normal incidence. Thus, for measurements of reflectivity vs angle, additional instrumentation, including a receiving hydrophone, must be mounted separately from the submarine. Such a package would have to be deployed separately and buoyed up from the bottom. However, the additional information available at oblique incidence is valuable enough for us to discuss it here, despite these instrumental problems.

Measurements of reflectivity as a function of the angle of incidence should show multiple peaks corresponding to the different waves excited in the porous sediment; the angular position of those peaks should indicate the sound velocity of the wave to which it corresponds. To see this, we consider Eqs. 2.9, 2.10, and 2.11 (Brekhovskikh, 1960, Eqs. 4.18, 4.25, 4.26). These describe the reflection coefficient for a wave incident from fluid onto a solid capable of supporting both a transverse and a longitudinal wave. While they do not include the effect of the two longitudinal waves found in porous media, we can infer some of

the qualitative effects of multiple waves in porous media upon the reflectivity coefficient. These equations are

$$V = \frac{z_{2\ell} \cos^2 \theta_{2t} + z_{2t} \sin^2 \theta_{2t} - z_1}{z_{2\ell} \cos^2 \theta_{2t} + z_{2t} \sin^2 \theta_{2t} + z_1} \quad (2.9)$$

for the reflection coefficient where the impedances are

$$z_1 = \frac{\rho_1 c_1}{\cos \theta_1}, \quad (2.10a)$$

$$z_{2\ell} = \frac{\rho_2 c_2}{\cos \theta_{2\ell}}, \quad (2.10b)$$

$$z_{2t} = \frac{\rho_2 b_2}{\cos \theta_{2t}},$$

and Snell's law is given by

$$\frac{\sin \theta_1}{c_1} = \frac{\sin \theta_{2\ell}}{c_2} = \frac{\sin \theta_{2t}}{b_2}. \quad (2.11)$$

As before, the subscript 1 indicates the fluid medium of the incident wave and subscript 2 the solid medium of the refracted waves. The subscripts ℓ and t refer to longitudinal and transverse waves, so that θ_{2t} is the direction of the refracted transverse wave, measured relative to the surface normal. c_2 is the longitudinal wave velocity, while b_2 is the transverse one.

Let us consider what happens to $|V|$ as θ_1 is increased from zero. c_2 will generally be greater than b_2 so that the critical

angle corresponding to the longitudinal wave is encountered first. At this angle $\theta_{2\ell} = 90^\circ$, $Z_{2\ell}$ becomes infinite and $|V| = 1$ giving the first peak (actually a cusp). For θ_1 greater than this critical angle, $Z_{2\ell}$ is imaginary, and $|V|$ decreases from 1, since the real parts of the numerator and denominator in the V equation are not equal. If b_2 is less than c_1 , there will be no second peak in V . However, if b_2 is greater, then at some θ_1 , $\theta_{2t} = 90^\circ$, $\sin^2\theta_{2t}/\cos\theta_{2t} = 4 \sin^2\theta_{2t} \cos\theta_{2t} = 0$, and $|V| = 1$, since the imaginary parts of the numerator and denominator are equal, as are the real parts (except for sign). For θ_1 greater than this second critical angle, both Z_{2t} and $Z_{2\ell}$ are imaginary, θ_{2t} complex and both $\sin^2\theta_{2t}$ and $\cos^2\theta_{2t}$ real, so that $|V| = 1$. Thus, $|V|$ reaches a second maximum at the second critical angle. Substituting the critical angles in Snell's law, together with $\theta_{2t} = 90^\circ$ or $\theta_{2\ell} = 90^\circ$ as appropriate, gives the sound velocities b_2 and c_2 .

A similar peaking in $|V|$ can be expected when the three waves of porous media are present, except that there should be three peaks, permitting as above the determination of the three sound velocities. However, this development has ignored attenuation. The effect of attenuation is to reduce V below 1 except at $\theta_1 = 90^\circ$; the peaks will be flattened somewhat and possibly obliterated if the attenuation is high enough (Brekhovskikh, 1960, Fig. 8, p. 20; MacKenzie, 1960, various figures).

These ideas are applicable to the Modular Acoustic System, since its transducer mount is trainable in azimuth and elevation. Provided attenuation is not too great (and prior to actual measurements we cannot really say how large it will be), the sound velocities of the three can be determined by observing the three peaks.

These velocities in turn are relatable to the characteristics of the porous medium (density and elasticity terms), and hence to the effects of the tubes. Since parameters of the porous medium will differ from site to site as the tubes and their density change, changes in the structure of reflectivity vs angle can be expected.

In addition, dramatic effects should occur for those cases (e.g., small pogonophorans) where the characteristic frequency is within the band of the Modular Acoustic System. Figures 11 and 12 of Biot (1956b) show the changes in the two longitudinal velocities with frequency. Comparing a measurement of reflectivity vs angle at two different frequencies, provided they were near f_c , should show a shift in the location of the peaks. In fact, for some frequencies, the longitudinal wave of the second kind might have a wave velocity less than that of the water, so the third peak might not occur. As frequency is raised and the phase velocity increases, the third peak might appear as the velocity exceeded that of water.

2.7 Spherical Wave Modifications to the Plane Wave Approximation

The reflectivity coefficients discussed above are computed using a plane wave approximation. However, in many experiments ALVIN might be so near the bottom that this approximation would not be valid. We are then required to consider the modifications to the theory of reflectivity when the wave front is spherical. This situation may occur in many practical instances, since one of ALVIN's special advantages is its ability to come close to areas of interest.

As in so much of this work, Brekhovskikh's presentation is the most complete and physically instructive (1960, Chap. IV).

The spherical wave is expanded into a set of plane waves, both homogeneous and inhomogeneous (the latter implying attenuation with depth), and the reflection coefficient determined. The reflection coefficients computed from plane wave theory are correct for the spherical waves except near critical angles, provided $\omega R_1/c_1$ is much greater than 1, where R_1 is the distance from the point of specular reflection on the surface to the receiver. This is generally easy to attain even for the lowest frequency of the system, 2 kHz; for a R_1 value of 2 m, $\omega R_1/c_1 = 16.8$.

Brekhovskikh gives a correction term to the reflection coefficient $V(\theta_1)$ (1960, Eqs. 19.36, 19.37) which is

$$i/2[V''(\theta_1) + V'(\theta_1) \cot\theta_1]/(\omega R_1/c_1) . \quad (2.12)$$

This is generally small so that we can use the plane wave reflection coefficient to describe the medium. However, at the critical angle, V'' is large; if the solid is lossless, V'' will be infinite, since V has a cusp at the critical angle.

Fortunately, Brekhovskikh has reexamined the approximation leading to the correction term cited above by carrying out another approximate solution valid in the vicinity of the critical angle (1960, Sec. 22, Eqs. 22.19, 22.20).

This work yields a more precise statement of how close θ_1 can be to the critical angle $\theta_1(\text{crit})$ and still have the plane wave reflection coefficient be valid. This statement is

$$(\omega R_1/c_1) [\theta_1 - \theta_1(\text{crit})]^2 \gg 1 \quad (2.13)$$

and is valid for θ_1 both less than and greater than the critical angle. If we consider 10 to be much greater than 1, and if θ_1 is no closer than 2° to the critical angle, then R_1 must be 980 m at 2 kHz and 44 m at 45 kHz. If the deviation exceeds 5° , R_1 must be at least 156 m at 2 kHz and 7 m at 45 kHz.

If this condition is not satisfied, then the reflected energy is *not* described by the plane wave reflection coefficient. The correct reflection coefficient is (Brekhovskikh, Eq. 22.19)

$$V = 1 - \frac{4c_1 \rho_1 e^{i\pi/8}}{c_2 \rho_2 \Gamma(\frac{1}{4}) (\frac{\omega}{2c_1} R_1)^{\frac{1}{4}}} \left[\frac{\pi}{\sin 2\theta_1(\text{crit})} \right]^{\frac{1}{2}} \left(1 + \frac{i n^2}{2} + \dots \right) \quad (2.14)$$

where

$$n = \left(\frac{2\omega}{c_1} R_1 \right)^{\frac{1}{2}} \sin \frac{[\theta_1 - \theta_1(\text{crit})]}{2} \quad (2.15)$$

At an angle of incidence equal to the critical angle ($n = 0$), the reflection coefficient is reduced from 1 as shown by the second term in the equation above, arising from the creation of the lateral wave, which propagates along the surface but attenuates quickly with depth. For this second term to be ignored $(\omega R_1 / 2c_1)^{\frac{1}{4}}$ must be much greater than 1. This is a far more stringent condition than that imposed earlier that $\omega R_1 / c_1$ be much greater than 1. For $(\omega R_1 / 2c_1)^{\frac{1}{4}}$ to be equal to 10, R_1 must be 2390 m at 2 kHz and 106 m at 45 kHz.

These considerations show that we *must* consider the spherical nature of the wave front in evaluating reflection coefficients

near critical angles in many cases where ALVIN is within 100 to 1000 m of the reflecting surface. This need not be a disadvantage. For instance, at $\eta = 0$ we could carry out a sequence of experiments, varying either range (R_1) or frequency (ω) and observe the variation in reflection coefficient predicted by Eq. 2.14. A regression fit to the data would then yield the impedance ratio

$$\frac{\rho_1 c_1}{\rho_2 c_2}$$

There is the possibility of an interesting theoretical investigation if one were to incorporate the effects of attenuation in Brekhovskikh's approach. For instance, his Eqs. 19.36 and 19.37, cited earlier, break down because of singularities in V' and V'' ; attenuation removes the cusps from the V curves and hence eliminates the singularities. Under these conditions, the plane wave approximation may be valid much closer to the critical angle than is predicted for the lossless case.

2.8 The Layer Thickness Created by Tube-Building Marine Organisms

The thickness of the porous layer created by tube-building marine organisms may vary from a few centimeters to a maximum of a few meters for the largest species. The wavelength in water of the frequencies of the Modular Acoustic System vary from 0.75 m (2 kHz) to 3.3 cm (45 kHz). Thus, the porous layers must be viewed as thin layers, which nonetheless can be expected to have an effect on the reflection properties of the bottom. If all tubes stop suddenly at some depth, an unlikely occurrence, then there will be a discontinuous change in the properties of the sediment, and the layer will be like a thin film such as found in quarter- and half-wave plates, resulting in interference effects. It is more likely

that the population of tubes will vary with depth resulting in a continuous change in the sediment properties. If this variation is slow enough, the WKB approximation will hold; this states that the medium is understandable within the framework of geometrical optics, and that the sound rays will be refracted, but not reflected, as they penetrate the sediment. If the population varies radically at various depths, there will be some reflection from each depth increment, the amount of reflection being heavily dependent on the shape of the sound velocity profile and angle of incidence (Brekhovskikh, 1960, Chap. III, esp. Figs. 76, 77). This reflected energy will be in addition to that from the interface. Prior to acoustic measurement and a more detailed understanding of tube population with depth, we cannot say which approach is appropriate. Brekhovskikh provides the theoretical framework for each of these models. However, closed solutions are possible for only a very limited set of profiles, so that it may not be possible to model the actual situation as exactly as one might wish.

2.9 Determination of the Reflection Coefficient

The reflection coefficient is defined as the fraction of the incident energy of a plane wave that is returned as a second plane wave in the specular direction. The plane wave is a wave of infinite extent in both space and time. The problems arising from the spherical nature of actual wavefronts were discussed previously. There are additional problems arising from a combination of the short pulse length of the incident acoustic energy and the beam-pattern of the transducer. This results in the actual insonified area being a function of both incident angle and of time. Since

beam pattern is a function of frequency, the insonified area will vary with frequency as well. These geometric factors must be taken into account if reflectivity is to be computed accurately. Urick (1967, p. 195) gives a formula appropriate for grazing incidence. The more general case of arbitrary incidence is not easily determined analytically, but can be computed numerically. Urick and Hoover (1956) give useful nomograms as functions of distance from the surface, pulse length and transducer beamwidth and axis angle.

2.10 The Mechanical Properties of Sediments

There is an alternative approach to the effects of tubular inclusions in sediments. Using a self-consistent approximation for the energy of crack and needle inclusions in a solid matrix, various investigators (Walpole, 1969; Wu, 1966; Budiansky and O'Connell, 1975; O'Connell and Budiansky, 1974) have computed the modifications to the elastic constants created by the inclusions. The work of O'Connell and Budiansky is the most recent and most complete.

All these efforts are "DC" approaches which ignore the motion of fluid in the pores and the effects of frequency. However, since they are formulated in terms of the elastic constants, they provide a good base for a study of the mechanical (also called geotechnical) properties of the sediments.

O'Connell (1975) has computed *cross-over frequencies*, above which fluid in one crack or tube is unable to transfer to another crack or tube. The transfer mechanisms he considered are (1) passage of the fluid through the permeable solid between cracks

and (2) passage at the intersection of cracks. In both cases, he estimates the frequency to be in the range of 1 to 10 kHz (the range of our Modular Acoustic System); although he feels the calculation is inexact, so that these frequencies could be off by one or even two orders of magnitude. Whatever the value of the cross-over frequency, it is a demarcation of frequency regions where attenuation mechanisms differ, and hence is a frequency where reflectivity could change. We await the publication of his work for possible inclusion with, and modification to, the theories of Biot described above.

This work also suggests combined geotechnical and acoustic measurements, where the geotechnical parameters are measured by mechanical means and the longitudinal and transverse wave velocities are determined acoustically. These acoustically determined velocities could then be compared with those computed from the geotechnical measurements.

2.11 Experimental Sites

The choice of specific sites in which to examine the acoustic effects of marine organisms on the sediments is difficult because of the limited information on densities in the deep sea. If a study of the effect of a particular species is desired, the depth range in which it is found can be determined from Menzies, George, and Rowe (1973), who discuss faunal geographic patterns extensively. However, this text cannot be counted on to provide an exact latitude and longitude where densities are high. Such determinations must come from the personal experience of individual benthic ecologists, based on their sampling of the deep. The areas which we mention below are based mainly on conversations with benthic

experts at Woods Hole Oceanographic Institute and should be viewed only as examples.

Rowe (1975) told us of an area, east of Hudson Canyon in 2000 to 3000 m of water, which has the appearance of a fossil shallow-water mud flat. Tubes of high density stand vertically off the bottom like organ pipes. The animals now living in them are not those that would have created them. The area is fossilized in the sense of being a *fossil community*, since the substrate itself is not rock, but indurated clay. The tubes are about a centimeter in diameter and up to 50 cm long. There is some question about how representative this area is; it may be an old salt marsh, although its microfauna is not characteristic of near-shore environments. But whether this kind of fossil community is widespread in the ocean or localized, this might be a very productive area to examine, since the density of tubes is high. Note that for this area the characteristic frequency is well below the operating range of the Modular Acoustic System. One possible problem in making good measurements would be the degree of surface roughness, which would cause energy loss through scattering.

Rowe also noted the presence of *Homolampus*, a sea urchin, along the eastern continental rise. It burrows to a depth of 2 ft; however, its density may be too low to be important. The same might be said of *Molpadia*, a sea cucumber, which is found in the 2000- to 3000-m range and buries up to 20 cm deep (Rhoads and Young, 1971). Rowe also suggested the means of carrying out a more controlled experiment by killing the fauna in an area and baiting it to attract opportunistic species. After an appropriate wait, one would measure the acoustic effects on the sediment and compare these with measurements made before the baiting. Since

Hyalinoecia feeds on carcasses, one can generate a *Hyalinoecia* colony in this way (Fauchald, 1975), provided the baiting is carried out within the depth ranges where *Hyalinoecia* is typically found.

Grassle (1975) felt that the areas described in a recent paper (Grassle *et al.*, 1975) which lie along the Gay Head-Bermuda transect would provide a variety of environments where the sediments were modified in different ways. Over a depth range of 400 to 2000 m, they observed densities of macrofauna in the range of 1,000 to 8,000 per sq m, based on dredge samples. These exist only in the top 1 to 2 cm of the sediment. In the same depth range, the megafauna, counted in photographs, showed densities of 0.03 to 3.5 in the same area (Table 3 of Grassle *et al.*, 1975). Since the Gay Head-Bermuda transect has been so extensively studied, it is appealing to consider acoustic measurements in these areas. However, the depth range of the macrofauna may be too small and the density of the megafauna too low for significant effects. Conversely, there is always the possibility of higher-than-average concentrations at some sites; in fact Grassle *et al.* observe and discuss the patchiness in distributions.

More specifically, Grassle *et al.* note concentrations of *Hyalinoecia artifex* at 500 m and large numbers of the burrowing cerianthid anemone at 1500 and 1800 m. (This anemone is 1/2- to 3/4-in. in diameter and approximately 5 in. long.)

Incidentally, Grassle *et al.* observe another unusual bottom condition that would be worth examining acoustically, although it is not a tunneling effect. The brittle star, *Ophiomusium*

lymani, occurs within the depth range of 1700 to 2170 m and arranges itself in a regular pattern relative to its nearest neighbor, so that much of the bottom is covered by these animals.

Finally, Grassle (1975) mentioned another possible area. His colleagues, Hessler and Jumars, have done recent work in the San Diego trough and have observed large densities of balls of mud about 2 in. to 3 in. in diameter. These balls have many tubules created by a cirratulid polychaete worm that lives within the ball. The tubules might be quite small in diameter since the worm itself is small - 2 to 3 mm in length. In general, the San Diego trough might be an excellent place to carry out the kinds of experiments we have been discussing, since it is a region of higher animal densities than the Gay Head-Bermuda transect (Grassle *et al.*, 1975, Table 4 and 5).

High densities of pogonophorans are found in the Malay archipelago (Ivanov, 1963, p. 128) and the Kurile-Kamchatka trench (Godeaux, 1974), both of which are well outside the usual range of ALVIN's operations. Sampling of pogonophorans along the east coast of the United States has occurred only within the last 10 years (Southward and Brattegard, 1968), but there is no information on densities.

2.12 Supplemental Instrumentation

Meaningful acoustic experiments must be coupled with sampling and study of the benthic community and a characterization of the sediment. There are two types of devices, box cores and photography, for sampling the benthos that have immediate applicability for comparison with acoustic measurements. They will provide information on tube diameter, length, and population density as a function of depth.

A Birge-Ekman box core, 15×15 cm, was acquired for ALVIN under the ARPA grant and used successfully in the Gulf of Maine and the Tongue of the Ocean (Rowe *et al.*, 1972a,b). Grassle (1975) feels that the RUM core, which is a box core 20×20 cm, is the largest size that can be presently used on ALVIN for meaningful penetration into the substrate. A special platform called SCAMP, being developed for attachment to ALVIN, will permit the submersible to be anchored to the bottom. With SCAMP, the large spade core described by Hessler and Jumars (1974) could be deployed directly from the submersible. This core is $1/2$ m on a side and is capable of taking relatively undisturbed samples.

Rhoads and Cande (1971) have built a *special camera* that photographs the sediment structure as a clear wedge is slowly forced through the sediment. Striking pictures of relatively undisturbed burrows, tubes, and fecal remains are taken. Although this device has been used only in shallow water, Grassle (1975) informs us that Rhoads has designed a deep-water version.

The detached receiver needed to carry out reflectivity measurements as a function of angle is briefly described below, although it is not our purpose to give a complete design specification.

The height of the receiver above the bottom should be controllable from ALVIN, so as to carry out measurements near the critical angle as a function of R_1 . It should be broadband and omnidirectional, relying on the source transducer to provide the directionality. It might have its own recording system, or, more preferably, be connected by cable to ALVIN. (This would require careful negotiation and preplanning with ALVIN personnel.)

Since maintenance of the proper geometry is essential in these experiments, ALVIN's acoustic navigation system should be employed.

2.13 Conclusions

In this section, we have considered measurements of reflectivity from marine sediments both as a function of angle and of frequency. The discussion has been focused on the experimental consequences of the porosity created by tube-building marine organisms, although a number of the points (such as the attention one must pay to the spherical nature of the wavefront) apply to any measurements of bottom properties made from ALVIN.

Some measurements, particularly those made vs frequency, could be made with the Modular Acoustic System and ALVIN alone. Others, such as measurements of reflectivity vs angle, require the implementation of additional instrumentation, not yet designed.

REFERENCES, SEC. 2

Aller, R.C. and R.E. Dodge (1974). "Animal-Sediment Relations in a Tropical Lagoon - Discovery Bay, Jamaica," *J. Marine Res.* 32:209-232.

Bezrukov, P.L. and A. Romankevich (1960). "Stratigraphy and Lithology of the Sediments in the Northwest Pacific Ocean," *Dokl. Akad. Nauk SSSR* 130:417-420, cited in Seilacher (1964), p. 305.

Biot, M.A. (1956a). "Theory of Propagation of Elastic Waves in a Fluid-Saturated Porous Solid. I. Low-Frequency Range," *J. Acoust. Soc. Am.* 28:168-178.

Biot, M.A. (1956b). "Theory of Propagation of Elastic Waves in a Fluid-Saturated Porous Solid. II. Higher Frequency Range," *J. Acoust. Soc. Am.* 28:179-191.

Biot, M.A. (1962a). "Mechanics of Deformation and Acoustic Propagation in Porous Media," *J. Appl. Phys.* 33:1482-1498.

Biot, M.A. (1962b). "Generalized Theory of Acoustic Propagation in Porous Dissipative Media," *J. Acoust. Soc. Am.* 34:1254-1264.

Brekhovskikh, L.M. (1960). *Waves in Layered Media* (Academic Press, New York).

Budiansky, B. and R.J. O'Connell (1975). "Elastic Moduli of a Cracked Solid." Submitted for publication.

Carlisle, D.B. (1963). Comments appearing in Ivanov (1963) (q.v.), pp. v, ix.

Condon, E.U. and H. Odishaw (1967). *Handbook of Physics* (McGraw-Hill, New York), p. 3-13.

Fager, E. (1964). "Marine Sediments: Effects of a Tube-Building Polychaete," *Science* 143:356-359.

Fauchald, K. (1975). Alan Hancock Foundation. Personal communication via Miss Charlene Long of Bolt Beranek and Newman Inc.

Galaitsis, A.G. and K.U. Ingard (1973). *Studies of Sound Absorption and Attenuation of Sound in Ducts* (Massachusetts Institute of Technology, Cambridge).

Godeaux, J.E.A. (1974). "II. Phylum Pogonophora," in *Chemical Zoology, Volume VIII*, M. Florkin and B. Scheer, Eds. (Academic Press, New York), pp. 25-26.

Grassle, J.F. (1975). Woods Hole Oceanographic Institution. Personal communication.

Grassle, J.F., H.L. Sanders, R.R. Hessler, G.T. Rowe, and T. McLellan (1975). "Pattern and Zonation: A Study of the Bathyal Megafauna Using the Research Submersible ALVIN," *Deep-Sea Research* 22:457-481.

Hamilton, E.L. (1974). "Geoacoustic Models of the Sea Floor," in *Physics of Sound in Marine Sediments*, L. Hampton, Ed. (Plenum Press, New York), pp. 181-221.

Hessler, R.R. and P.A. Jumars (1974). "Abyssal Community Analysis from Replicate Box Cores in the Central North Pacific," *Deep-Sea Research* 21:185-209.

Hyman, L.H. (1959). *The Invertebrates, Volume 5: The Smaller Coelomate Groups* (McGraw-Hill, New York), pp. 208-227.

Ivanov, A.V. (1963). *Pogonophora* (Academic Press, London).

MacKenzie, K.V. (1960). "Reflection of Sound from Coastal Bottoms," *J. Acoust. Soc. Am.* 32:221-231.

Menzies, R.J., R.Y. George, and G.T. Rowe (1973). *Abyssal Environment and Ecology of the World Oceans* (John Wiley and Sons, New York).

Morse, P.M. and K.U. Ingard (1968). *Theoretical Acoustics* (McGraw-Hill, New York), pp. 252-270.

Noiseux, D.U., N.B. Noiseux, and Y. Kadman (1975). "Development, Fabrication, and Calibration of a Porous Surface Microphone in an Aerofoil," Bolt Beranek and Newman Inc., Report No. 3014.

O'Connell, R.J. and B. Budiansky (1974). "Seismic Velocities in Dry and Saturated Cracked Solids," *J. Geophys. Res.* 79:5412-5426.

O'Connell, R.J. (1975). Harvard University, Personal communication.

Rhoads, D.C. (1963). "Rates of Sediment Reworking by *Yoldia limatula* in Buzzards Bay, Massachusetts, and Long Island Sound," *J. Sedimentary Petrology* 33:723-727.

Rhoads, D.C. and D. J. Stanley (1965). "Biogenic Graded Bedding," *J. Sedimentary Petrology* 35:956-963.

Rhoads, D.C. (1967). "Biogenic Reworking of Intertidal and Subtidal Sediments in Barnstable Harbor and Buzzards Bay, Massachusetts," *J. Geology* 75:461-476.

Rhoads, D.C. and D.K. Young (1970). "The Influence of Deposit-Feeding Organisms on Sediment Stability and Community Trophic Structure," *J. Marine Res.* 28:150-178.

Rhoads, D.C. and D.K. Young (1971). "Animal-Sediment Relations in Cape Cod Bay, Massachusetts. II. Reworking by *Molpadia oolitica* (Holothuroidea)," *Marine Biology* 11:255-261.

Rhoads, D.C. and S. Cande (1971). "Sediment Profile Camera for *In Situ* Study of Organism-Sediment Relations," *Limnology and Oceanography* 16:110-114.

Rowe, G.T. (1971/1972). "The Exploration of Submarine Canyons and Their Benthic Faunal Assemblages," *Proc. Roy. Soc. (Edinburgh)* (B) 73:159-169.

Rowe, G.T., P.H. Wiebe, J.M. Teal, and K.L. Smith (1972a). "Development of Equipment for Use in Deep-Ocean Biological Research," in *Technical Progress Report, Advanced Marine Technology, 1 Feb 71 - 31 July 71, WHOI-72-33*, A.E. Maxwell (Woods Hole Oceanographic Institution, Woods Hole, Mass.) pp. 38-40 and Fig. 11.

Rowe, G.T., P.H. Wiebe, J.M. Teal, and K.L. Smith (1972b). "Development of Equipment for Use in Deep-Ocean Biological Research," in *Technical Progress Report, Advanced Marine Technology, 1 Aug 71 - 31 Jan 72, WHOI-72-90*, A.E. Maxwell (Woods Hole Oceanographic Institution, Woods Hole, Mass.) pp. 63, 65.

Rowe, G.T. (1974). "The Effects of the Benthic Fauna on the Physical Properties of Deep-Sea Sediments," in *Deep-Sea Sediments - Physical and Mechanical Properties*, A. Inderbitzen, Ed. (Plenum Press, New York), pp. 381-400.

Rowe, G.T. (1975). Woods Hole Oceanographic Institution. Personal communication.

Seilacher, A. (1964). "Biogenic Sedimentary Structures," in *Approaches to Paleoecology*, J. Imbrie and N. Newell, Eds., pp. 296-316.

Southward, E.C and T. Brattegard (1968). "Pogonophora of the Northwest Atlantic: North Carolina Region," *Bull. Marine Science* 18:836-875.

Stoll, R.D. (1974). "Acoustic Waves in Saturated Sediments," in *Physics of Sound in Marine Sediments*, L. Hampton, Ed. (Plenum Press, New York), pp. 19-39.

Urick, R.J. (1954). "The Backscattering of Sound from a Harbor Bottom," *J. Acoust. Soc. Am.* 26:231-235.

Urick, R.J. and R.M. Hoover (1956). "Backscattering of Sound from the Sea Surface: Its Measurements, Causes, and Application to the Prediction of Reverberation Levels," *J. Acoust. Soc. Am.* 28:1038-1042.

Urick, R.J. (1967). *Principles of Underwater Sound for Engineers* (McGraw-Hill, New York).

Walpole, L.J. (1969). "On the Overall Elastic Moduli of Composite Materials," *J. Mech. Phys. Solids* 17:235-251.

Wigley, R.L. and K.O. Emery (1967). "Benthic Animals, Particularly *Hyalinoecia* (Annelida) and *Ophiomusium* (Echinodermata), in Seabottom Photographs from the Continental Slope," in *Deep-Sea Photography*, J.B. Hersey, Ed. (Johns Hopkins, Baltimore), pp. 235-249, esp. Figs. 22-3 and 22-4.

Wu, T.T. (1966). "The Effect of Inclusion Shape on the Elastic Moduli of a Two-Phase Material," *Int. J. Solids Structures* 2:1-8.

3. SPECTRAL MEASUREMENTS OF GROUPS OF A SINGLE SPECIES OF FISH

3.1 Introduction

The deep scattering layer is a pervasive phenomenon found in most of the world's oceans. As such, it can be a problem to active detection systems in many environments. The United States Navy has expended considerable sums both in making direct measurements of deep scattering layer acoustic properties, and in sampling fish which make up the layer. The combined acoustic and biological experiments have had a long-term goal: determining their relationship, so that a measurement of one might serve as a predictor of the other.

An entirely analogous problem occurs in fisheries' science. The National Marine Fisheries Service has the responsibility of monitoring and assessing fish resources, so that proper fishing limits may be determined. The usual methods of fish stock assessment are faunal sampling and monitoring of commercial landings. Acoustic techniques, if suitably refined, are a logical way of increasing the efficiency of the Service in its assessment task.

These combined acoustic and biological measurements have been complicated by the extraordinary complexity of the experimental situation, especially in the deep scattering layer; often tens of different fish species may be present at a given site. In this section, however, we discuss measurements at sites where typically groups of only one species are found.

Over 80% of the migrating species making up the deep scattering layer possess swim bladders (Marshall, 1971, 1960), which as resonant systems (NDRC, 1946) result in not only pronounced structure in spectral measurements of the acoustic returns scattered

from the fish, but also far stronger returns than would occur from the fish alone, if they had no bladders. This structure can be related to the internal pressure in the bladder, the bladder's radius and distortion from spherical shape, and various energy loss mechanisms in the bladder's gas and the surrounding fish tissue (Weston, 1967).

Thus, there is a relationship between the physiology of a fish and the acoustic spectra of sound reflected from that fish. As each species of fish possesses its own unique physiology, this relationship may be species specific. Establishing the specificity of this relationship between spectral and physiological features of a single species of fish requires a number of measurements on groups of fish, preferably of one size, known to be predominantly of one species. Since laboratory stress may change the characteristics of larger species (e.g., anesthetizing fish may relax musculature and hence change bladder size and stiffness), and since deep scattering layer species rarely survive sampling, it is preferable to carry out these measurements in the natural environment.

3.2 Theoretical Background

3.2.1 Bladder equations for a single fish

The theoretically derived formulas for swim-bladder resonance display the relationship between the frequency dependence of the swim-bladder's scattering cross section and physiological parameters, such as bladder size and shape and characteristics of the surrounding tissue. Weston's review article (1967) provides many of these formulas.

Using his Eqs. 39 through 47, the bladder scattering cross section, σ_s , is

$$\sigma_s(f) = 4\pi R^2 \left[\left(1 - \frac{f_0^2}{f^2} \right)^2 + \frac{1}{Q_s^2} \right]^{-1} \quad (3.1)$$

where the resonant frequency, f_0 , is

$$f_0 = (2\pi R)^{-1} \left(\frac{3\gamma P_0 + 4\mu_1}{\rho} \right)^{\frac{1}{2}} \quad (3.2)$$

and the resonant-system Q , determined by the loss mechanisms, is

$$Q_s^{-1} = Q_r^{-1} + Q_t^{-1} + Q_f^{-1} \quad (3.3)$$

The three components of Q_s^{-1} are the radiation damping, Q_r^{-1} , the thermal damping in the gas within the bladder, Q_t^{-1} , and the damping due to shear motion in the fish tissue surrounding the bladder, Q_f^{-1} .

$$Q_r^{-1} = k_b R \quad (3.4)$$

$$Q_t^{-1} = \frac{9\gamma^{\frac{1}{2}} P_0 (\gamma-1)}{\rho \omega_0^2 R^3} \sqrt{\frac{v}{2\omega_0}} \quad (3.5)$$

$$Q_f^{-1} = \frac{4\mu_1 \mu_2}{\rho \omega_0^2 R^2} \quad , \quad (3.6)$$

where R is the bladder radius, γ is the ratio of specific heats of the gas at constant pressure and constant volume, P_0 is the

ambient pressure, ρ is the water density, $\mu_1(1+i\mu_2)$ is the complex shear modulus of the fish tissue, k_0 is the wave vector corresponding to the resonant frequency, and ν' is the thermal diffusivity of the gas.

Modifications in the resonant frequency for a prolate spheroid are given by Eq. 13 of Weston (1967), where constant volume is assumed:

$$f_e/f_0 = 2^{\frac{1}{2}} e^{-1/s} (1-e^2)^{\frac{1}{4}} \left\{ \frac{\ln[1+(1-e^2)^{\frac{1}{2}}]}{1-(1-e^2)^{\frac{1}{2}}} \right\}^{-\frac{1}{2}} ; \quad (3.7)$$

e is the ratio of the major and minor axes of the spheroid.

He also discusses the modifications for other shapes.

3.2.2 Group effects

A measurement at sea examines fish grouped either into aggregations, such as the deep scattering layer, or into more ordered schools. The acoustic returns from such groups are usually analyzed to yield the volume scattering strength, $S_v(f)$, which is the target strength of a unit volume of water. $S_v(f)$ can be determined from experimental quantities, such as range, received sound pressure level, and send and receive sensitivity, in accord with the formalism found in Urick (1967). A particular application of that formalism is found in McElroy and Wing (1971).

Volume scattering strengths are related to the scattering cross sections by the formula

$$S_v(f) = 10 \log_{10} \sum_s n_s \sigma_s(f) / 4\pi , \quad (3.8)$$

where n_s is the average number of fish per unit volume of a particular species and size and varies from 10^{-3} to $10/m^3$ in deep scattering layers (Backus *et al.*, 1968). Since n_s is a function of position in the water volume, $S_v(f)$ will generally be a function of range from the measuring transducer. In addition, since measurement systems never insonify just a unit volume of water, the $S_v(f)$ determined experimentally will be an average over the actual insonified volume, which is determined by pulse length and beam pattern.

$S_v(f)$ is the measured quantity and $\sigma_s(f)$ is the quantity descriptive of an individual fish. If we are to relate the acoustic and the physiological measures of a fish species, we must choose an area where the average $S_v(f)$ measured by an acoustic system (such as the Modular Acoustic System) is determined by only one value of $\sigma_s(f)$, that is, by an insonified volume of only one species and one size.

The determination of layers where only one species occurs is possible (Sec. 3.5), but restriction to only one size is impossible. We substitute a requirement of as small a spread in fish size as possible. This spread in size results in a spread in bladder radius, resonant frequency (Eq. 3.2), and scattering cross section (Eq. 3.1). If the spread is small, the $\sigma_s(f)$ determined from $S_v(f)$ will look very similar to that described by Eq. 3.1 for the scattering cross section, except that we will have an effective Q_g^{-1} for the group (Weston, 1967), rather than the Q_s^{-1} for a single individual appearing in Eq. 3.1. Thus, Q_g^{-1} will be larger than Q_s^{-1} , corresponding to a further flattening in the resonance curve described by Eq. 3.1. It should be possible to infer Q_s from Q_g if the fish in the group are sampled and their size distribution determined.

If the size range of fish of one species is not small (as would occur if both juveniles and adults were present), or if a number of species are present (as occurs in most deep scattering layers), then $S_v(f)$ will contain more than one resonance peak, and/or individual peaks will be broadened so much that it is meaningless to talk of a single resonance and a group Q_g . Under these circumstances, identification of structure in $S_v(f)$ with individual species becomes far more difficult, if not impossible.

These points emphasize the desirability of selecting experimental areas where just one species with a small range in size is found.

3.2.3 Depth dependence

In addition to the effects of species and size on resonant frequencies, there can be a spreading caused by the dependence of resonant frequency on depth (the P_0 term in Eq. 3.2). An acoustic pulse will insonify some depth range as a result of pulse length and transducer beam width. However, the Modular Acoustic System mounted on a submersible allows minimization of these effects, since layers and schools of fish can be closely approached. This closeness permits shorter pulse lengths for a detectable return and a smaller depth range insonified for a given beamwidth. Submersibles, such as ALVIN, also permit measurement of scatterers when they are at their greatest depth. Under those circumstances, the depth range insonified by the sonar results in the smallest relative range in P_0 , and, hence, in the smallest possible variation in f_0 .

3.2.4 Multiple scattering

The determination of volume scattering strength mentioned above (Urick, 1967) presupposes that multiple scattering is negligible; that is, the energy incident on any given scatterer is only that from the source and not from nearby scatterers re-radiating energy. However, if fish are densely schooled, the reradiated energy can be significant. For instance, in the Slope Water (Huntsman, 1924; Iselin, 1936), where the layers of *Ceratostomelus maderensis* sometimes coalesce into schools, the density can reach as high as $10/m^3$, rather than the more usual $10^{-3}/m^3$ in scattering layers (Backus *et al.*, 1968). This higher figure implies a mean spacing of fish of about 0.4 m. Two questions must then be asked: (1) Is the reradiated power at a fish from its neighbors significant compared to the direct power from the source, and (2) Is the reactive part of the reradiated field, which at close range can exceed the resistive part, of significance?

In considering the first question, let us suppose there are two fish (numbered 1 and 2) at about the same range, r_0 , from the source which has source level p_0 at 1 m. Then, the level at fish No. 1 and at fish No. 2, due to the source (0) are the same and are

$$p_{10} = p_{20} = \frac{p_0}{r_0} \quad . \quad (3.9)$$

The pressure at fish No. 2 caused by that pressure reradiated from fish No. 1 is

$$p_{21} = \frac{p_1}{r_{12}} \quad , \quad (3.10)$$

where p_1 is the pressure at 1 m, which has been reradiated from fish No. 1, and r_{12} is the range from fish No. 1 to fish No. 2. p_1 is easily estimated using the scattering cross section σ_s , and the incident power on fish No. 1.

$$\frac{p_{10}^2}{\rho c} \times \frac{\sigma_s}{4\pi} = \frac{p_1^2}{\rho c} \quad (3.11a)$$

or

$$p_1 = \frac{p_{10}}{2\sqrt{\pi}} \sqrt{\sigma_s} \quad (3.11b)$$

Comparing the pressure at fish No. 2 reradiated from fish No. 1 with that direct from the source, we get

$$\frac{p_{21}}{p_{20}} = \frac{p_1/r_{12}}{p_0/r_0} = \frac{p_{10}\sqrt{\sigma_s}/r_{12}}{2\sqrt{\pi} p_0/r_0} = \frac{\sqrt{\sigma_s}}{2\sqrt{\pi} r_{12}} \quad (3.12)$$

Considering the worst case, when σ_s is maximum at resonance ($f=f_0$), Eq. 3.1 gives,

$$\sigma_s = 4\pi R^2 Q_s^2 \quad (3.13)$$

Q_s is estimated to be about 6 (Weston, 1967, p. 73). R , the gas bladder radius, will be estimated from a knowledge that gas bladders occupy about 5% of the volume of fish (Marshall, 1971, 1960) and that at the particular site we are considering, the fish are about 65 mm long (Backus *et al.*, 1968), which implies a displacement volume of about 2.5 cc (Krueger *et al.*, 1975). R is then

computed from the equation,

$$\frac{4}{3} \pi R^3 = 0.05 \times 2.5 ; \quad (3.14)$$

$R = 0.31$ cm. Combining these numerical values, we get for the ratio of reradiated to direct pressure,

$$p_{21}/p_{20} = \frac{RQ_s}{r_{12}} = \frac{0.31 \times 10^{-2} \times 6}{0.4} = 0.047 . \quad (3.15)$$

Having determined the relative contribution from one fish to the field about another, we can consider the effect of all fish surrounding the one in question. In a spherical shell of radius r and thickness Δr about the fish, the number of reradiating fish, ΔN , is

$$\Delta N = 4\pi r^2 \Delta r n_s , \quad (3.16)$$

where n_s = the number per unit volume = $10/m^3$.

Since the energy reradiated from one fish at distance r compared to the direct energy is given by the square of Eq. 3.12, that due to ΔN fish is

$$4\pi r^2 \Delta r n_s \frac{\sigma_s}{4\pi r^2} = n_s \sigma_s \Delta r . \quad (3.17)$$

Power is summed, rather than pressures, since the reradiated energies are incoherent from fish to fish. The total relative power at the fish in question is given by the integral of Eq. 3.17.

$$\int_0^{r_0} n_s \sigma_s dr = n_s \sigma_s r_0 , \quad (3.18)$$

where r_0 is given by the size of the school or layer for long pulses, or by the pulse length for shorter ones (that is, short compared to school dimensions). For a pulse of length τ , power reradiated from the fish in a sphere of radius $r_0 = c\tau/2$ will at least partially overlap at the fish located at the center of the sphere. We then have for the reradiated power at the center of the sphere compared to the direct power, the following expression, using Eqs. 3.13 and 3.18

$$n_s \sigma_s r_0 = n_s 4\pi R^2 Q_s \frac{c\tau}{2} \quad . \quad (3.19)$$

Using the numbers appropriate for *Ceratoscopelus maderensis* in the Slope Water schools reported by Backus *et al.* (1968), this is

$$\begin{aligned} n_s 4\pi R^2 Q_s \frac{c\tau}{2} &= 10 \times 2 \times \pi \times (0.31 \times 10^{-2})^2 \times 6 \times 1500 \times \tau \\ &= 5.4 \tau \quad . \quad (3.20) \end{aligned}$$

Multiple scattering can then be ignored for pulse lengths, τ , such that this number is small. For instance, if $\tau = 1$ msec, it is 0.005 and for 10 msec, it is 0.05. However, a pulse of 100 msec would not be short in this context.

The second question is concerned with a comparison of the far field radiated from a source (normally called the resistive part) and the near field or reactive portion. Equations 7.1.5 and 7.1.7 of Morse and Ingard (1968) show that the ratio of the reactive to the resistive portions of the radiated field from both monopoles and dipoles is $1/kr$, where k is the wave vector and r the distance. If we set $r = 0.4$ m, $1/kr$ is 0.12 at 5 kHz and 0.03 at 20 kHz. While we had to consider the entire school

in determining the resistive portion of the reradiated field above, we need only consider nearest neighbors to the fish in question when examining the reactive part, because of its faster falloff with range. There will be 6 to 10 nearest neighbors, each contributing a relative resistive portion of the field of about 0.047 (Eq. 3.15). The reactive portion, relative to the direct, from all 10 is then (adding powers as above),

$$10 \times (0.047)^2 \times (0.12)^2 = 0.0003 \text{ at } 5 \text{ kHz and}$$
$$0.00002 \text{ at } 12 \text{ kHz.}$$

These small numbers show we may ignore the reactive component.

3.3 Experimental Background

Experimental confirmation of spectral structure due to gas bladder resonances exists both in controlled laboratory experiments and in at-sea experiments. Batzler and Pickwell (1971) have measured spectral returns from large individual fish in a pressure chamber that display a resonance peak and its shift to higher frequencies with increasing pressure. McCartney and Stubbs (1971) have similar results. Comparisons with the fish found in deep scattering layers have not yet been made, as these species have a very poor survival rate when brought to the surface and captured. Obviously, experiments conducted from a submersible are not subject to such problems.

At-sea broadband measurements have displayed resonance peaks attributable to gas-bladdered fish (Chapman and Marshall, 1966; McElroy, 1974). A particularly careful study by Hersey, Backus, and Hellwig (1962) followed the change in frequency of the peaks

as individual deep scattering layers moved up and down in accord with diurnal migration patterns. Two types of layers were identified. In one type, resonant frequency varied as the 1/2 power of the ambient water pressure occurring at the depth of the layer; this variation corresponded to individual specimens of fish in that layer that maintained their gas bladders at constant volume by adding gas as they descended. The second type of layer showed a 5/6th power dependence on ambient pressure, which corresponded to a constant gas content in the bladder of individual specimens of fish, regardless of layer depth.

These two types of layers, exhibiting two types of resonant-frequency variation with depth, obviously correspond to two radically different physiological mechanisms occurring in the fishes making up the layers. In the first, each fish must add or subtract gas from the bladder as it migrates vertically. Kanwisher and Ebeling (1957) claim that, in spite of the evidence that such a phenomenon must occur, the fish cannot attain the rates of gas exchange required. In the second, the bladder is inflated and deflated, but is restricted to the size range available to it within the fish.

This, then, is the type of physiological question which could be examined in a combined acoustic- and biological-sampling experiment performed where a single species is present.

3.4 Application of the Modular Acoustic System to Spectral Measurements of the Deep Scattering Layer

It should be possible to measure the resonant shape of scattering cross sections for fishes of the deep scattering layer grouped either in layers or in schools, using the spectral

capabilities of the Modular Acoustic System. The System's directional transducers can be scanned through frequency ranges of about 3 to 1. These directional transducers are better suited to picking out a smaller oceanic volume than the omnidirectional sources usually used in spectral work; these small volumes are desirable to minimize the broadening of resonance curves created by a range in pressures, as discussed in Sec. 3.2.3.

By making these measurements repetitively during the diurnal migration as ALVIN rises or descends with a layer, the dependence of resonant frequency on depth can be determined. The Modular Acoustic System, operating under computer control, can quickly scan frequency; a given spectrum can be measured within a 5-min. period so that reasonably rapid changes can be monitored. Spectral resolution can be changed during an experiment to display structure as finely as needed, based on observations of the spectra made in the submersible during a given dive.

Sampling and observation of the layer can be carried out in the course of the same dive discussed in Sec. 3.6.

There are additional considerations that must be addressed in implementing these experiments. One arises from the change in insonified volume as frequency, and hence beamwidth is changed. This change will blur the data somewhat, since the depth range insonified will vary with frequency.

In addition, the experimenter must insure that the insonified volume under examination for frequency dependence lies completely within the layer of fish. If it does not, then a changing fraction of this volume will be actually scattering energy as frequency

(and hence beamwidth) is changed; the result will be structure more attributable to the beamwidth than to the targets of interest. The closer the experimenter is to the target layer, the less likely he is to examine a volume in which some portion contains no fish. How close he must be is determined by the depth of the layer or the size of the school. In the Slope Water, some schools are sufficiently large (100 m across) to allow the submersible to approach closely enough to insonify an individual school without disturbing the fish.

Others, however, are so small (10 m across) (Backus *et al.*, 1968), that a close approach is not possible. An alternative, under this circumstance, is to make the measurements from a much greater range, so that the sound beam insonifies many similar schools. Then, as frequency and hence insonified volume is changed, the average density of fish will stay nearly constant. The disadvantage of this alternative is that the beamwidth will result in a greater depth range of fish being insonified than occurs for measurements close to schools, and, hence, an undesirable spread in resonant frequency. Experimenters should be prepared for either the small- or large-school condition before arriving at an experimental site. Both sizes of school are encountered in the Slope Water.

3.5 Experimental Sites

While deep scattering layers are found throughout the world's oceans, the problem is to locate those particular areas where a single species, limited to a small size range, can be found. We discuss a number of such areas of different character.

The Slope Water. The Slope Water of the western Atlantic extends from Cape Hatteras to the Grand Banks and exhibits its own temperature-salinity characteristics and coloration, distinct from the continental shelf to the west and the Gulf Stream to the east (vonArx, 1962). A most striking feature is the special characteristic of the deep scattering layer; unlike any other region of the deep ocean (except off Newfoundland), the components of the DSL are grouped into dense schools during the daytime, rather than existing in a diffused layer (Backus *et al.*, 1968). Further, only one species has been found in these schools; Backus *et al.* found individuals of the species *Ceratoscopelus maderensis* ranging in length from 52 to 73 mm (mean size 62.4 m, a standard deviation of 2.9 mm). *Ceratoscopelus maderensis* has a well-developed swim bladder.

The fish density in the schools is high, but probably not high enough to introduce significant multiple scattering as discussed in Sec. 3.2.4.

The fact that fish in the Slope Water are clustered into schools rather than dispersed in diffuse layers imposes restraints on the relative position of the submarine during acoustic measurements, as discussed in Sec. 3.4. This problem is counterbalanced by the relative ease in sampling the fish from the submersible (discussed below).

There is at least one unpredictable aspect to this proposed area. The dense schooling of *Ceratoscopelus maderensis* in the Slope Water does not occur every year. For unknown reasons, there are times when the schools are very small or nonexistent (Backus, 1974).

The Cariaco Trench. The Cariaco Trench is an oceanic region north of Venezuela where the deep scattering layer at 250 m is composed principally of the myctophid fish, *Diaphus taanini* Norman, (Baird *et al.*, 1974). Baird *et al.* found only small numbers of *Steindachneria argentea* Goode and Bean and juvenile *Bregmaceros nectabanus* in addition to the *Diaphus*. The *Diaphus*, which has a well-developed gas bladder, were all of nearly the same size: average standard length of 40.7 mm, with a standard deviation of 2.7 mm. The density of *Diaphus* was estimated by Baird *et al.* at 2 per 1000 m³. Populations in the Trench can in general be expected to be low, on the basis of Baird's work and that of earlier investigators (Mead, 1963). However, they are high enough to have been observed acoustically as deep scattering layers (Baird *et al.*, 1974).

In deeper, anoxic water containing hydrogen sulfide, Baird *et al.* (1973) have found another layer, also seemingly of just one species - *Bregmaceros nectabanus* Whitley. This might be a particularly interesting layer to study in combined acoustic and physiological experiments, because of the adaptions *Bregmaceros* must have made to survive in a hostile environment.

The San Diego Trough. Barham (1971) has reviewed an extensive series of submersible dives he has made in the San Diego Trough to observe the deep scattering layer. His observations are visual and did not involve captures of the observed specimens to permit positive identification. However, he is a highly skilled observer of midwater fishes, so that even his visual impressions have a high probability of being correct. On p. 102, he noted observations of swarms of a silver-scaled myctophid (tentatively

identified as *Myctophum aurolaternatum*). On p. 104, he notes observations of 273 myctophids in one dive. Between Costa Rica and Acapulco, Mexico he observed dense swarms of myctophids, probably *Benthosema panamense*, so numerous that some lodged in the submersible superstructure.

The implication is that there are regions of the San Diego Trough where reasonable densities of single species are likely to occur. Detailed location of such sites require both the advice of a skilled observer, such as Barham, and attention to season of the year so that only adults, rather than a mix of adults and juveniles, would occur.

General Observations Made by James Craddock. Craddock (1975) discussed with us his observations and intuitions, based on an extended period of sampling the deep scattering layer and on the reports of his colleagues. He is convinced that individual layers will often contain single species and that densities of the fish will be higher than many observers expect. Specific examples he cited are:

1. *Diaphus dumerili* is caught in large numbers by the National Marine Fisheries Service off Cape Hatteras.
2. Milliman and Manheim (1968) observed large densities of a small fish off Hatteras. Craddock surmises (based on the Fisheries' experience) that it was *Diaphus dumerili*, though he admits no sure identification was possible under the circumstances.
3. Craddock has found 300 individuals of *Diretmus argenteus* in the stomach of a porpoise. Obviously, they must have schooled for this to have occurred.

4. Gerhardt Krefft has told Craddock of a catch of 15 tons of one species of myctophid off the east coast of South America (2° to 5° N) within the last 5 years. This catch was taken with the huge nets of the Walther Herwig. Other species were not found in significant numbers.

5. *Benthosema glaciale* make up 95% of the catch taken in sampling of the deep scattering layer in northern waters off Labrador. *Benthosema* is caught in large numbers.

Controlled Experiments. The National Marine Fisheries Service (Beaumariage, 1975) is conducting a controlled experiment in 1975 at Jeffries Ledge, where specific species of commercial fish are released into a net and then observed acoustically, both individually and in aggregations. Such single-frequency measurements could profitably be supplemented by measurements over a range of frequency.

3.6 Fish Identification and Sampling

One of the justifications for using ALVIN as a platform from which to make acoustic measurements of the deep scattering layer is the possibility of precise identification of the species contributing to the scattering. If the sampling is carried out from the surface, using nets deployed from a surface ship, there is concern that the fish one has measured acoustically are not the same as those sampled. In some cases, where an entire area contains only one species and size, this concern is of less importance than in others, such as the Cariaco Trench, where other species are known to be present. Even in the Slope Water, where the schools are made up seemingly of only one species, other species are present in other layers (Backus, 1975).

These problems are resolved to a degree by two procedures:

1. Insuring that a trained observer is present in the submersible during the acoustic measurements and insuring that he has the opportunity to identify the measured layer by looking at it through a porthole. Barham (1971) observes that the fish seemed less disturbed if the submersible rose or descended through the schools or layers than if it navigated horizontally through them.

2. Actually sampling the layer measured acoustically by closing it with a net mounted on the submersible. Backus *et al.* (1968) collected large numbers (774) of specimens of *Ceratoscopelus maderensis* in the Slope Water with a very simple net. In this area, the density of fish was unusually high. With normal scattering layer densities, small simple nets cannot be expected to get a very representative sample. An attempt should be made to mount as large a net as possible, consistent with the constraints imposed by the submersible's small size. It is the view of ALVIN's chief pilot (Wilson, 1975) that such a net should be mounted aft (when the Modular Acoustic System is mounted forward) and rigged so it could be swung down once ALVIN is launched. The actual design of the sampling net requires careful coordination with ALVIN operating personnel. Should the best efforts at increasing net size be insufficient, surface sampling would have to be employed. However, even surface sampling would be preferable to an operation carried out entirely from the surface, since a trained observer accompanying the dive would insure that the species sampled was the same as that observed and measured acoustically.

Mention should be made of the plankton sampler designed by Wiebe (1972a,b) under the ARPA ALVIN contract. This is a submersible version of the Longhurst-Hardy plankton recorder, which

maintains a time record of sampling by collecting the plankton on a gauze sheet that is transported across the back end of the net. However, the net opening is small enough that it could not be expected to collect representative samples of mesopelagic fishes of the type making up the deep scattering layer, except in the special Slope Water circumstances of high density we have cited.

3.7 Conclusions

Because of the importance of the effect of fish of the deep scattering layer on sonar operations and because acoustic techniques are important to assessment of commercial species of fish, experiments designed to relate the acoustic returns from a fish to the physiological characteristics of the fish have both governmental and commercial interest. Such experiments would be more profitably carried out in the open sea than in laboratory experiments which subject fish to stress.

The Modular Acoustic System's spectral capability can be applied to this problem. Spectral structure in the scattering cross section of a fish as a result of its gas bladder is relatable to its physiology. Shifts in the structure peaks with changing depth of the fish have additional physiological implications.

Successful implementation of such experiments requires experimental conditions as controlled as nature allows. Sites should be chosen where only one species of nearly one size are examined.

REFERENCES, SEC. 3

Backus, R.H., J.E. Craddock, R.L. Haedrich, D.L. Shores, J.M. Teal, and A.S. Wing (1968). "Ceratoscopelus maderensis: Peculiar Sound-Scattering Layer Identified with this Myctophid Fish," *Science* 160:991-993.

Backus, R.H. (1974, 1975). Woods Hole Oceanographic Institution. Personal communication.

Baird, R.C., D.F. Wilson, and D.M. Milliken (1973). "Observations on *Bregmaceros nectabenus* Whitley in the Anoxic, Sulfurous Water of the Cariaco Trench," *Deep-Sea Res.* 20:503-504.

Baird, R.C., D.F. Wilson, R.C. Beckett, and T.L. Hopkins (1974). "Diaphus taanungi Norman, the Principal Component of a Shallow Sound-Scattering Layer in the Cariaco Trench, Venezuela," *J. Marine Res.* 32:301-312.

Barham, E.G. (1971). "Deep-Sea Fishes: Lethargy and Vertical Orientation," in *Proc. Int. Symp. on Biological Sound Scattering in the Ocean*, G. Brooke Farquhar, Ed. (U.S. Government Printing Office, Washington, D.C.), pp. 100-118.

Batzler, W.E. and G.V. Pickwell (1971). "Resonant Acoustic Scattering from Gas-Bladder Fishes," in *Proc. Int. Symp. on Biological Sound Scattering in the Ocean*, G. Brooke Farquhar, Ed. (U.S. Government Printing Office, Washington, D.C.), pp. 168-179.

Beaumariage, D. (1975). MUST Office, NOAA. Personal communication.

Chapman, R.P. and J.R. Marshall (1966). "Reverberation from Deep Scattering Layers in the Western North Atlantic," *J. Acoust. Soc. Am.* 40:405-411.

Craddock, J. (1975). Woods Hole Oceanographic Institution. Personal communication.

Hersey, J.B., R.H. Backus, and J. Hellwig (1962). "Sound Scattering Spectra of Deep Scattering Layers in the Western North Atlantic," *Deep-Sea Res.* 8:196-210.

Huntsman, A.G. (1924). "Oceanography," in *Handbook of Canada, British Association for the Advancement of Science, Toronto Meeting August 1924* (U. Toronto Press, Toronto), pp. 274-290, esp. 276-280.

Iselin, C. O'D. (1936). "A Study of the Circulation of the Western North Atlantic," in *Papers in Physical Oceanography and Meteorology*, Vol. 4 (Massachusetts Institute of Technology and Woods Hole Oceanographic Institution, Cambridge, Mass.), pp. 2-101.

Kanwisher, J. and A. Ebeling (1957). "Composition of the Swim-bladder Gas in Bathypelagic Fishes," *Deep-Sea Res.* 4:211-217.

Krueger, W.H., M.J. Keene, and A.A. Keller (1975). "Midwater Fishes of the Deepwater Dumpsite," Final Report to the National Oceanic and Atmospheric Administration (University of Rhode Island). Preprint. *Ceratoscopelus maderensis* entry in Appendix Table I.

Marshall, N.B. (1960). *Swimbladder Structure of Deep-Sea Fishes in Relation to their Systematics and Biology*, Discovery Reports, Vol. 31 (Cambridge University Press, Cambridge, England).

Marshall, N.B. (1971). "Swimbladder Development and the Life of Deep-Sea Fishes," in *Proc. Int. Symp. on Biological Sound Scattering in the Ocean*, G. Brooke Farquhar, Ed. (U.S. Government Printing Office, Washington, D.C.), pp. 69-73.

McCartney, B.S. and A.R. Stubbs (1971). "Measurements of the Target Strength of Fish in Dorsal Aspect, including Swimbladder Resonance," in *Proc. Int. Symp. on Biological Sound Scattering in the Ocean*, G. Brooke Farquhar, Ed. (U.S. Government Printing Office, Washington, D.C.), pp. 180-211.

McElroy, P.T. and A. Wing (1971). "Scattering Returns in the Mediterranean and Eastern Atlantic - Data and Instrumentation," in *Proc. Int. Symp. on Biological Sound Scattering in the Ocean*, G. Brooke Farquhar, Ed. (U.S. Government Printing Office, Washington, D.C.), pp. 220-231.

McElroy, P.T. (1974). "Geographic Patterns in Volume-Reverberation Spectra in the North Atlantic between 33° and 63° N," *J. Acoust. Soc. Am.* 56:394-407.

Mead, G.W. (1963). "Observations on Fishes Caught over the Anoxic Waters of the Cariaco Trench, Venezuela," *Deep-Sea Res.* 10: 733-734.

Milliman, J.L. and F.T. Manheim (1968). "Observations in Deep-Scattering Layers off Cape Hatteras," *Deep-Sea Res.* 15:505-507.

Morse, P.M. and U. Ingard (1968). *Theoretical Acoustics* (McGraw-Hill, New York), pp. 306-314.

National Defense Research Council (1946). *Physics of Sound in the Sea* (Department of the Navy, U.S. Government Printing Office, Washington, D.C., reprinted in 1969), pp. 460-477.

Urick, R.J. (1967). *Principles of Underwater Sound for Engineers* (McGraw-Hill, New York), pp. 187-194.

vonArx, W.S. (1962). *Introduction to Physical Oceanography* (Addison-Wesley, Reading, Mass.), pp. 312-320.

Weston, D.E. (1967). "Sound Propagation in the Presence of Bladder Fish," in *Underwater Acoustics, Vol. 2*, V.M. Albers, Ed., (Plenum Press, New York), pp. 55-88.

Wiebe, P.H. (1972a). "Development of Equipment for Use in Deep-Ocean Biological Research," in *Technical Progress Report, Advanced Marine Technology, 1 Feb 71 - 31 July 71, WHOI-72-33*, A.E. Maxwell (Woods Hole Oceanographic Institution, Woods Hole, Mass.), pp. 36-37 and Figs. 1-8.

Wiebe, P.H. (1972b). "Development of Equipment for Use in Deep-Ocean Biological Research," in *Technical Progress Report, Advanced Marine Technology, 1 Aug. 71 - 31 Jan. 72, WHOI-72-90*, A.E. Maxwell (Woods Hole Oceanographic Institution, Woods Hole, Mass.), pp. 46-47.

Wilson, V. (1975). Woods Hole Oceanographic Institution. Personal communication.

4. MICROTOPOGRAPHY AND SCATTERING

4.1 Introductory Comments

Deviations of a surface from complete flatness determine the scattering of energy from that surface at angles in addition to that of the specular reflection. Many measurements of scattering of acoustic energy from the ocean bottom are carried out under conditions where the characteristic roughness of the bottom is unknown. The roughness parameters are inferred from scattering data on the basis of a model that may not be correct. Urick (1967) stated that there were few data on roughness power spectra of ocean bottoms. More recently, Clay and Leong (1974) describe their own inferences of bottom roughness, based solely on echo sounding data. Their work emphasizes the desirability of knowing the bottom roughness explicitly. Luyendyk's (1969) measurement of the roughness spectrum with the Scripps' vehicle, Deep Tow, is one of the few instances where this roughness has been directly measured.

The direct tie between bottom roughness parameters due to the microtopography and the scattering of acoustic energy as a function of both angle and frequency strongly suggests carrying out an experiment where both measurements are made in a single area. The Modular Acoustic System has this capability, as we discuss below.

4.2 Theoretical Background - Scattering

Rather than outline the numerous theories of sound scattering, we will only discuss the results of two theories which present the important physical concepts and parameters. The theories are

Preceding page blank

those of Morse and Ingard (1968) and Clay and Leong (1974). The latter theory uses a more precise set of assumptions for measurements in the ocean than those found in Morse and Ingard.

The scattered intensity from a surface of area A_0 in the x-y plane is given by Eqs. 4.1 through 4.4 (Morse and Ingard, 1968, Eqs. 8.3.4 and 8.3.12), provided the distance R_1 of the receiver from the surface is large compared to the dimensions of the area A_0 *, and provided the maximum displacement of the surface is less than a wavelength.

$$I_s \approx 4\pi I_i \frac{A_0}{R_1^2} \left| \frac{\cos\theta_1 \cos\theta}{(\cos\theta_1 + \beta_0) (\cos\theta + \beta_0)} \right|^2 k^4 \gamma^4 |Z(k\gamma)|^2 , \quad (4.1)$$

where I_i is the incident intensity; θ_1 is the incident angle, and θ is the scattered angle, both measured relative to the normal to the surface; β_0 is the surface admittance; and k is the wave vector. γ is an angular function involving the components of the incident and scattered directions in the x-y plane and is defined by

$$\gamma^2 = \frac{1}{k^2} (\mu_x^2 + \mu_y^2) , \quad (4.2a)$$

where

$$\mu_x = k(\sin\theta_1 \cos\phi_1 - \sin\theta \cos\phi) \quad (4.2b)$$

*We have eliminated variations in surface admittance in this presentation of the Morse and Ingard formalism, since they assume a point reacting surface, incorrect for the sea floor. A complete solution to the scattering problem should include these effects for surfaces of extended reaction (defined in Morse and Ingard, 1968).

$$\mu_y = k(\sin\theta_i \sin\phi_i - \sin\theta \sin\phi) . \quad (4.2c)$$

ϕ_i and ϕ are azimuthal angles in a system of polar coordinates, corresponding to the polar angles θ_i for the incident wave and θ for the scattered (Morse and Ingard, Figs. 8.7 and 8.9).

The characteristics of the bottom are contained in $Z(k\gamma)$, which is the two-dimensional spatial Fourier transform of the roughness parameter $\xi(\vec{r}_A)$. ξ is the deviation in the vertical direction of the surface from complete flatness at the point x_A, y_A on the bottom ($\vec{r}_A = \hat{x}_A i + \hat{y}_A j$). The power spectral density of $Z(k\gamma)$ can be computed from the Fourier transform of the correlation function for the bottom. That function is assumed to be Gaussian by Morse and Ingard and has the form

$$T_\xi(d) = \langle \xi^2 \rangle e^{-\frac{1}{2}(d^2/\omega_\xi^2)} , \quad (4.3)$$

where $\langle \xi^2 \rangle$ is the rms value of ξ over the area A_0 , d is a horizontal distance variable over which correlation is to be determined, and ω_ξ is the correlation length. Correlation length can be viewed as a characteristic distance over which correlation of the deviation ξ from flatness is significant.

Computing the spatial Fourier transform of Eq. 4.3 yields $|Z(k\gamma)|^2$ for inclusion in Eq. 4.1.

$$|Z(k\gamma)|^2 = \frac{1}{8\pi^3} \omega_\xi^2 \langle \xi^2 \rangle e^{-k^2 \gamma^2 \omega_\xi^2} . \quad (4.4)$$

Equations 4.1 through 4.4 contain the germ of an ocean-bottom experiment relating microtopography and scattering measurements

to be performed with the Modular Acoustic System. We measure the microtopography in an area A_0 by determining $\xi(\vec{r}_A)$ throughout the area as a function of the two horizontal coordinates, x_A and y_A . We then compute the mean-square value of ξ ($\langle \xi^2 \rangle$), and evaluate the spatial autocorrelation function $T_\xi(d)$ from the data. Assuming for the moment that $T_\xi(d)$ has a Gaussian form, the correlation length w_ξ can be determined. Equation 4.4 for $|Z(k\gamma)|^2$ immediately follows. Then Eq. 4.1 predicts the scattered intensity as a function of both angle (θ_i , θ , and γ) and frequency or wavenumber (k). The predicted scattering can then be compared directly with that measured to test the validity of the theory. For backscattered energy (the only type which the Modular Acoustic System can measure until additional instrumentation is implemented as described in Sec. 2.12), the angular functions in Eq. 4.1 simplify as follows:

$$\left| \frac{\cos\theta_i \cos\theta}{(\cos\theta_i + \beta_0) (\cos\theta + \beta_0)} \right|^2 = \frac{\cos^4\theta_i}{(\cos\theta_i + \beta_0)^4} \quad (4.5)$$

$$\gamma = 2 \sin\theta_i \quad . \quad (4.6)$$

While the theory from Morse and Ingard discloses some of the important parameters such as correlation length and mean-square height variation, it requires modification for the experimental conditions encountered in actual at-sea experiments. Clay and Leong (1974) provide an excellent review of these considerations, combining theory and experiment in a single paper. For instance, by examining the spectral data of Luyendyk (1969), they determine an empirical form for $T_\xi(d)$ and find it is better fit by a straight line than a Gaussian function (Clay and Leong, Eq. 3.6 and Fig. 3.4). For any actual shape of $T_\xi(d)$, $Z(k\gamma)$ can be determined by a spatial two-dimensional Fourier transform.

In addition, they reason that the scattered intensity will be proportional to the area A_0 (as indicated by Eq. 4.1) only if the scale of the roughness (which is given by the correlation length ω_ξ) is much less than the radius of the first Fresnel zone. That radius, r_F , is given by the formula

$$r_F = (\lambda R_1 / 2)^{1/2}, \quad (4.7)$$

where λ is the wavelength of the sound and R_1 is the range from source-receiver to the scattering surface. The radius of the first zone is clearly changed as R_1 is changed. For large R_1 , r_F will be much greater than ω_ξ and the scattering proportional to A_0 , but as R_1 is decreased, and r_F becomes of the order of ω_ξ , the surface will be coherent over the first Fresnel zone. Pressures rather than intensities will sum, resulting in a sharp increase in scattered energy in certain directions. This change from incoherent to coherent scattering can be measured with the Modular Acoustic System as ALVIN decreases its range (R_1) to the surface. Typical beam widths of the Modular Acoustic System will be larger than the first Fresnel zone for most distances. For instance, this is true at 35 kHz for $R_1 > 4.4$ m and at 3 kHz for $R_1 > 0.8$ m. Thus, an experiment examining the dependence of scattered intensity on area may be conducted for all R_1 greater than these limits.

The formalism of Clay and Leong (1974, App. I, Eqs. 17 - 29) is more detailed than that of Morse and Ingard. In addition to the correlation function $r_\xi(d)$ (Eq. 4.3), they consider the probability distribution function of surface heights in a simple form,

$$w_G = \frac{1}{\sqrt{2\pi}} e^{-\frac{\xi^2}{2<\xi^2>}}, \quad (4.8)$$

this function's modification for shadowing effects at small grazing angles, and a characteristic function C_2 determined by W_G and $T_\xi(d)$. C_2 , in turn, determines the scattered intensity. This more complicated formalism may be necessary in some experimental situations where that of Morse and Ingard does not provide a good match to the data.

By examining the broadening of echo sounder traces, Clay and Leong are able to set limits on $\langle \xi^2 \rangle^{1/2}$. In some areas, they estimate it to be less than one centimeter (1974, p. 380). This figure of 1 cm is then an upper limit on the vertical resolution one might seek, but it is a limit we are unlikely to attain (Sec. 4.5).

4.3 Determination of Microtopography from ALVIN

In any experiment, the first step is a determination of the small-scale topography. The problem is simply stated: knowing position in the horizontal plane (x_A, y_A) , what is the height $\xi(\vec{r}_A)$ and how does it vary as x_A and y_A change in a known way? This question can be answered in either a deterministic or a statistical way.

4.3.1 Deterministic measurement of $\xi(\vec{r}_A)$

x_A and y_A can be determined by the use of the ALVIN navigation system known as ALNAV. While the absolute position, x_A and y_A , are poorly given by this system, relative changes in x_A and y_A are given with far greater precision. A general discussion of this accuracy is found in Sec. 5.3.1, where we see that relative errors may be less than 1% in the center of a navigation net. Relative changes are all that are really important in determining spectral amplitudes vs wavevector in the horizontal

plane of the ocean bottom. Accuracies will be best for shorter wavelengths where the errors in relative position are least. Absolute errors will increase as wavelength increases, although relative errors will not increase to the same degree.

These high relative accuracies are possible along one track, but not in directions normal to a track. The accuracy in the normal direction is limited by the accuracy with which we can return to a given point in the ocean, since this determines how well we can define the separation of two nominally parallel tracks. As discussed in Sec. 5.3.1, this error will be 1.5 m at a minimum.

In many situations, this 1.5-m error would be unacceptably large. If so, the investigator should think of implementing the more precise navigational scheme discussed by Spindel in Hunt *et al.* (1974), which increases the accuracy in relative positions by two orders of magnitude using Doppler shift information. This would be a major development effort.

Alternatively, the statistical sampling scheme described in Sec. 4.3.2 could be employed in some situations.

The second part of the problem is determination of ξ once x_A and y_A are known. This can be accomplished acoustically by driving the high-band transducer of the Modular Acoustic System at its upper limit, about 45 kHz, while pointing it downward. Choice of the high frequency gives minimum beamwidth (about 6°) and minimum penetration into the sediment so the primary return will be only from the ocean-bottom interface.

The limit on the accuracy of this measurement of ξ is fixed by the accuracy with which relative changes in depth are known.

Obviously, we wish to measure the wiggles in the ocean bottom and not the apparent wiggles caused by ALVIN's depth fluctuations as it moves along its survey path. The depth meter on ALVIN has a readout accuracy of 1 m, which is far too large an error. In Sec. 4.5, we discuss a strain-gauge depth meter with standard deviation of 2.8 cm. Further instrumental developments will reduce this figure in time and hence improve the accuracy of the determination of ξ .

4.3.2 Statistical measurement of $\xi(r_A)$

Scattering measurements are modeled by statistical descriptions of the ocean bottom, as we saw in Sec. 4.2. These descriptors include correlation lengths (Eq. 4.3) and probability distribution functions of the height (Eq. 4.8). Under these circumstances, where statistical quantities are used, it is not necessary to carry out a precise navigational survey of the ocean bottom. It is necessary only to sample $\xi(r_A)$ along random straight-line paths. We must keep track of the horizontal separation between vertical soundings along a given path to determine the dependence on horizontal wavevector, but it is not necessary to know the actual location of the path within the area A_0 .

For a random sampling method to be meaningful, all parts of the area A_0 should be sampled equally. That is, if P_A is the probability of sampling a small area A within A_0 , P_A should be made nearly constant in value over the area A_0 by an intelligent choice of the sampling scheme.

We will describe one such scheme, compute P_A , and show how to select a portion of the area A_0 so that P_A can be as arbitrarily

close to constant as the investigator feels is necessary. The result is shown in Fig. 4.2, based on evaluation of an elliptic integral.

Our sampling area A_0 is a circle of radius r_0 . This could be set up by implanting a transponder or reflector at the circle center and then tracing a circle in the sediment with ALVIN as it maintains constant range to the transponder. This trace could be created either by ALVIN's skid or by trailing some sediment marker, such as bright pellets, from ALVIN's underside.

In sampling, ALVIN starts at the perimeter and steers a straight-line course (randomly chosen) until it encounters the other side of the circle. Height above the bottom and depth are measured, as discussed in Sec. 4.3.1. Distance along the path is determined by integration of a velocity meter mounted on ALVIN. For maximum precision, a Doppler bottom-bounce velocity meter should be installed. When the submersible encounters the far side of the perimeter, the operator queries a random number generator giving any angle in the range 0° to 360° with equal probability. This angle is added to the old course to give the new course; if the new course does not lie within the circle, 180° is subtracted.

This geometry is shown in Fig. 4.1, where the large circle is the area A_0 of radius r_0 , and r_A is the distance from the circle center to the small area A . The path along which ALVIN steers is given by the vector r from the point B on the perimeter. The angle ψ has an equal probability of having any value between -90° and $+90^\circ$, because of the random course selection procedure described in the prior paragraph.

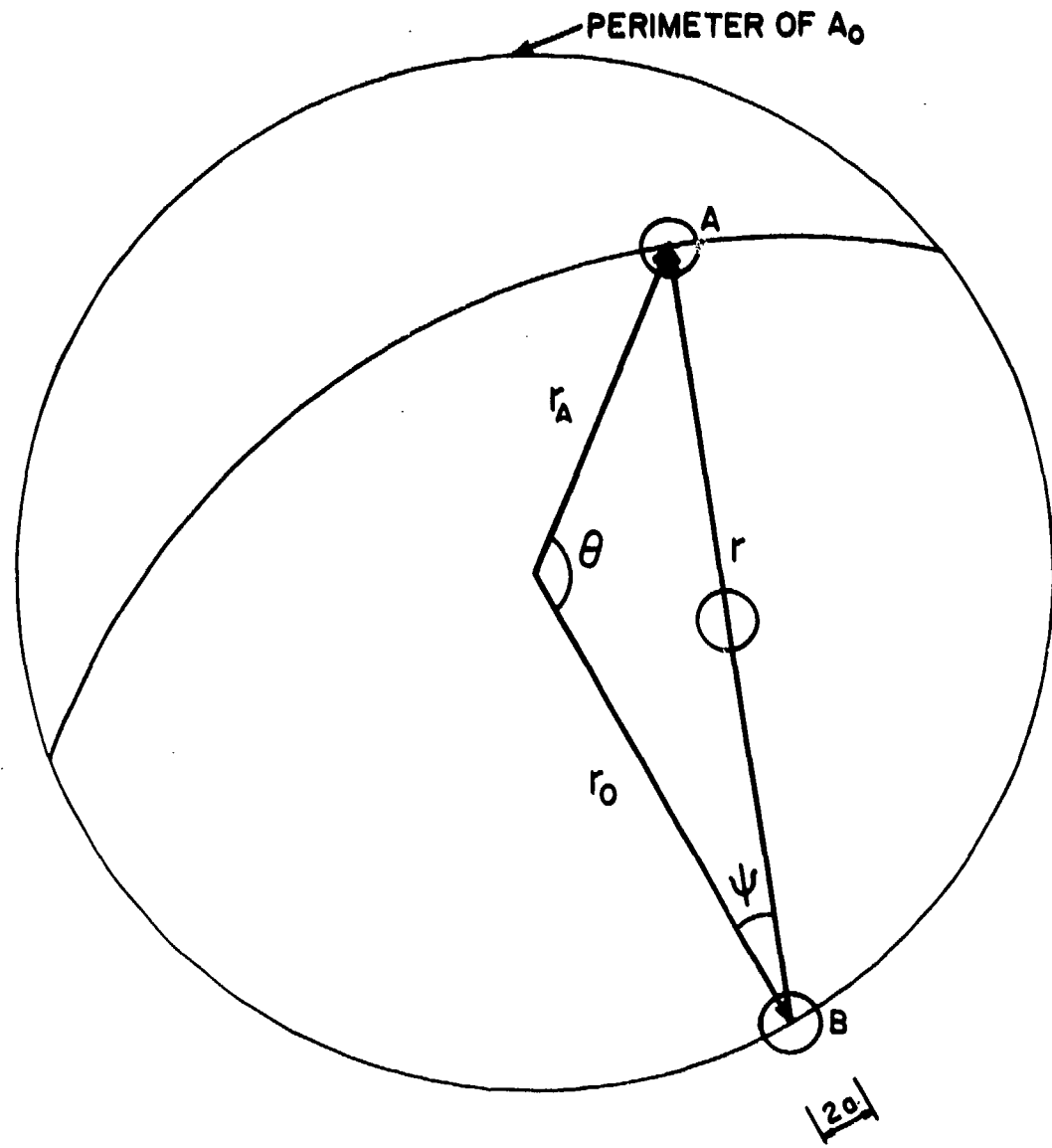


FIG. 4.1. GEOMETRY FOR STATISTICAL SAMPLING OF THE HEIGHT OF THE DEVIATIONS OF THE AREA A_0 FROM FLATNESS, $\xi(\vec{r}_A)$.

We ask first what is the conditional probability, P_{AB} , of intersecting area A if we start at B. We pose this problem a little more precisely by supposing we sample an area, also equal to A, under the submersible as it traverses its course along r (this is shown by the small circle part way along r). P_{AB} is then defined as the probability of the center of the area to be sampled lying anywhere within the sampling area under the submersible. If we define the radius of the area A as a , then P_{AB} is one for $0 \leq r \leq a$. For greater values of r , P_{AB} will fall off as $1/r$, since any direction is equally probable (ψ is random) and the arc length in an angular range $d\psi$ is proportional to r . P_{AB} then has the form

$$\begin{aligned} P_{AB} &= 1 & \text{for } 0 \leq r \leq a \\ &= a/r & r \geq a \end{aligned} \quad . \quad (4.9)$$

We found it necessary to pay special attention to the range r less than a to prevent the solution becoming infinite for $r_A = r_0$.

r is expressed in terms of the other quantities in Fig. 4.1, using a trigonometric identity (Dwight, 1957)

$$r^2 = r_0^2 + r_A^2 - 2r_0 r_A \cos\theta \quad . \quad (4.10)$$

The probability P_A can be calculated from P_{AB} by using the probability of B lying at a particular point on the perimeter. Calling this probability P_B , we observe that our sampling scheme is not predisposed to any particular position on the perimeter, so that $d(P_B)$, which is the probability of B lying in any incremental

angle $d\theta$, is independent of θ .*

$$d(P_B) \sim d\theta/2\pi . \quad (4.11)$$

By integrating over all the possible B positions, we get P_A , the probability of sampling area A.

$$P_A = \int_0^{2\pi} P_{AB} d(P_B) \sim \int_0^{2\pi} \frac{a}{(r_0^2 + r_A^2 - 2r_0 r_A \cos\theta)^{1/2}} \frac{d\theta}{2\pi} \quad (4.12)$$

for $r_A \leq r_0 - a$.

The integral (I) in Eq. 4.12 is transformed into an elliptic integral by the two sequential transformations,

$$x = \pi - \theta$$

and

$$\phi = \frac{x}{2} \quad (4.13)$$

$$I = \frac{a \cdot 2}{2\pi} \int_0^{\pi} \frac{d\theta}{(r_0^2 + r_A^2 - 2r_0 r_A \cos\theta)^{1/2}} = \frac{a}{\pi} \int_0^{\pi} \frac{dx}{(r_0^2 + r_A^2 + 2r_0 r_A \cos x)^{1/2}}$$

$$= \frac{2a}{\pi} \int_0^{\pi/2} \frac{d\phi}{(r_0^2 + r_A^2 + 2r_0 r_A - 4r_0 r_A \sin^2 \phi)^{1/2}} , \quad (4.14)$$

*The proportionality constant in Eq. 4.11 is given by the number of traverses by ALVIN. We have not as yet completed this part of the calculation; it is not necessary to our present calculation.

where we have used the identity $\cos 2\phi = 1 - 2\sin^2\phi$.

$$I = \frac{2a}{\pi} \frac{1}{r_0 + r_A} \int_0^{\pi/2} \frac{d\phi}{(1-k^2\sin^2\phi)^{1/2}} = \frac{2a}{\pi} \frac{1}{r_0 + r_A} K(k) , \quad (4.15)$$

where

$$k^2 = \frac{4r_0 r_A}{(r_0 + r_A)^2} , \quad (4.16)$$

and $K(k)$ is the complete elliptic integral (Jahnke and Emde, 1945), which is tabulated.

Finally, if we drop some of the additional proportionality factors, we get for P_A ,

$$P_A = K \left\{ \left[\frac{4r_0 r_A}{(r_0 + r_A)^2} \right]^{1/2} \right\} \cdot \frac{1}{(1+r_A/r_0)} \quad \text{for } r_A \leq r_0 - a . \quad (4.17)$$

In Fig. 4.2, we plot P_A at arbitrary radius r_A , compared to P_A at $r_A = 0$, namely,

$$\frac{P_A(r_A/r_0)}{P_A(0)} = \frac{K \left\{ \left[\frac{4r_A/r_0}{(1+r_A/r_0)^2} \right]^{1/2} \right\}}{K(0)} \cdot \frac{1}{1+r_A/r_0} , \quad (4.18)$$

which shows how well we sample an area at radius r_A , compared to the center of the circle.

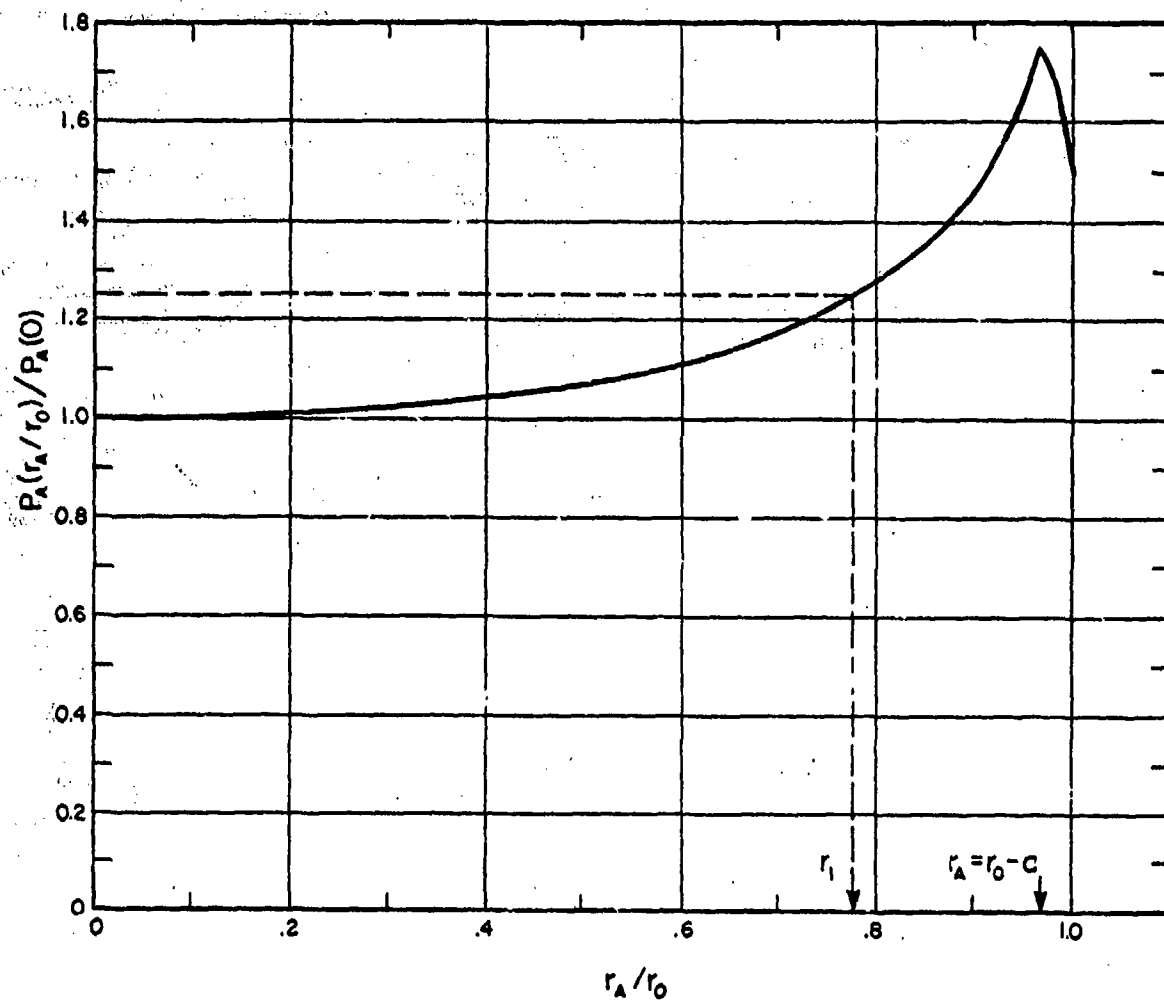


FIG. 4.2. PROBABILITY OF SAMPLING AN AREA A AT A DISTANCE r_A FROM THE CENTER (RELATIVE TO THE RADIUS OF THE SAMPLED AREA, r_0), NORMALIZED BY THE PROBABILITY OF SAMPLING AT THE CENTER ($r_A=0$). r_1 IS A RADIUS DEFINING AN AREA WITHIN THE SAMPLED AREA A, SUCH THAT THE NORMALIZED PROBABILITY LIES BETWEEN 1 AND 1.25.

For $r_0 \geq r_A > r_0 - a$, the elliptic integral of the first kind $F(\phi, \alpha)$ (Jahnke and Emde, 1945) is the result of the integration giving P_A . We have used F with a particular choice of a/r_0 to evaluate the probability for areas near the perimeter of the circle. The result is incorporated in Fig. 4.2. Equation 4.18 cannot be used for the entire r_A range since $K(1)$ is infinite.

Examination of Fig. 4.2 discloses how to select a portion of A_0 so the probability P_A is nearly constant. A second circle of radius r_1 is drawn within the larger circle of radius r_0 . As r_1 is decreased, the degree of constancy improves.

Operationally, one would select the area one wished to measure acoustically. This would dictate r_1 . r_0 is then selected, based on the degree of constancy in P_A which the investigator feels necessary. Both circles are marked on the sediment. The submersible then passes back and forth between the limits set by the circle A_0 , but measures ξ only within the smaller circle of radius r_1 .

Other random sampling schemes can be developed, consistent with the navigational abilities of ALVIN. Some may give even better constancy in P_A than we have attained here. Our purpose was to consider a specific useful example and develop the formalism. Note that our procedure presupposes isotropy in the roughness in the horizontal plane. Thus, it would be an inappropriate procedure to follow if the dominant structure was sand waves.

4.4 Scattering Measurements

Once the microtopography has been ascertained, either deterministically or statistically, a scattering measurement can be

carried out in the sampled area using the Modular Acoustic System. The System can be operated over a range of frequencies and over a full range of values of the angle of incidence by using the trainable transducer mount. Section 4.2 shows that scattered energy depends on both frequency and angle.

A first series of measurements should examine backscattering only, using ALVIN's common transmitter-receiver. Later measurements could examine scattering at other angles, using additional instrumentation deployed external to ALVIN (Sec. 2.12). Measurements at normal incidence to the bottom will contain reflected as well as scattered energy, so the investigator will wish to concentrate his measurements at other angles. Attention must be given to the area actually insonified, since this is dependent on pulse length and angle of incidence (Sec. 2.9).

The final result is a comparison of scattered energy and theoretical predictions, providing the basis for refinements both in the theory and the experimental procedures.

4.5 Supplemental Instrumentation

The need for instrumentation in addition to the Modular Acoustic System has been discussed in previous sections. These include the ALNAV navigation system for ALVIN and its refinements (Sec. 4.3.1), a velocity meter (Sec. 4.3.2), and a detached detector system for scattering measurements other than backscatter (Sec. 4.4). Details on these can be found elsewhere in this report (Secs. 2.12 and 5.3.1).

A critically important instrument is a *depth meter* capable of measuring relative changes in the submersible's depth during

sampling of the microtopography. A worthy candidate is the Plessey Environmental Systems Model 4026 Pressure Sensor. This is a strain gauge whose absolute accuracy and resolution have been enhanced by temperature compensation. Its depth range is 0 to 20,000 ft, with an absolute accuracy of ± 6 ft over a 30-day period. However, our concern is not with an absolute measure of depth, but in accurately monitoring relative depth changes. An indication of the resolution possible is contained in tests carried out in 1970 on this instrument for the US Naval Underwater Sound Lab, New London, Connecticut (Clausen, 1974).

The first test measured stability, based on more than 35 measurements of 4- and 2-sec averages of the depth reading when the gauge was statically loaded with weights. The standard deviation of the 4-sec averages was 0.045 psi, corresponding to 2.8 cm of depth. The standard deviation for 2-sec averages corresponded to 3.9 cm of depth. The standard deviation for other time-period averages can be computed by noting that the ratio of the variances [$1.93 = (3.9/2.8)^2$] is nearly equal to the inverse ratio of the two averaging times ($2 = 4/2$).

The second test measured resolution of a 0.5-psi change in pressure at the maximum pressure measured by the unit, 10,000 psi. By averaging 40 measurements of 4-sec averages of 10,030.0 psi and 10,030.5 psi, an average difference of 0.496 psi was determined. This is quite good, but the submersible is motionally unstable enough that unaveraged measurements would probably be required every 4 to 10 sec rather than every 160 ($= 4 \times 40$). Thus, the resolution is determined not by these longer averages but by the standard deviations determined in the stability test (this same

deviation was determined in the resolution test as well). Using two standard deviations as an estimate of the accuracy with which we measure relative changes in depth, we conclude that the Plessey Model 4026 can resolve changes of 6 cm or greater if 4-sec averages are used.

The state of the art may well have advanced since this system was tested in 1970. Before selecting an actual depth meter, it would be well to consider newer systems, particularly those made by Neil Brown Instrument Systems, Falmouth, Massachusetts.

4.6 Experimental Sites

There should be little difficulty in picking out many sites where the small-scale topography could be examined in the way described in this section.

A number of specific areas lie along the Gay Head-Bermuda transect, a region that has been studied extensively by benthic ecologists. Grassle *et al.* (1975) describe observations of the bottom topography and fauna made from ALVIN in a number of different depth ranges along this transect. For instance, they note an unusual small-scale relief, probably created by the red crab *Geryon quinquedens*: "Mounds and depressions, often with burrows, were everywhere. These mounds were up to a meter across, the largest being irregular in form and usually with several burrow openings."

4.7 Conclusions

Since microtopography of the ocean bottom and scattering of acoustic energy by the bottom have a direct relationship to

one another, it is logical to measure both quantities at a site as a test for particular scattering theories. The Modular Acoustic System can be used for both these tasks. The topography can be determined either directly, using the ALVIN navigation system to define the measurement geometry, or statistically. In either case, depth variations must be measured precisely. An interesting and varied set of sites, which have already been examined visually from ALVIN, lie along the Gay Head-Bermuda transect.

REFERENCES, SEC. 4

Clausen, G.N. (1974). Plessey Environmental Systems, San Diego, California. Personal communication via Mr. Hubert Wright, Bolt Beranek and Newman.

Clay, C.S. and W.K. Leong (1974). "Acoustic Estimates of the Topography and Roughness Spectrum of the Sea Floor Southwest of the Iberian Peninsula," in *Physics of Sound in Marine Sediments*, L. Hampton, Ed., (Plenum Press, New York), pp. 373-446.

Dwight, H.B. (1957). *Tables of Integrals and Other Mathematical Data*, 3rd Edition (MacMillan, New York), Formula 410.01.

Grassle, J.F., H.L. Sanders, R.R. Hessler, G.T. Rowe, and T. McLellan (1975). "Pattern and Zonation: A Study of the Bathyal Megafauna Using the Research Submersible ALVIN," *Deep-Sea Research* 22:457-481.

Hunt, M.M., W.M. Marquet, D.A. Moller, K.R. Peal, W.K. Smith, and R.C. Spindel (1974). "An Acoustic Navigation System," Technical Report WHOI-74-6 (Woods Hole Oceanographic Institution, Woods Hole, Mass.), pp. 60-63.

Jahnke, E. and F. Emde (1945). *Tables of Functions* (Dover, New York), pp. 73, 78, 52-54, 61-67.

Luyendyk, B.P. (1969). Ph.D. Thesis at University of California, La Jolla, California, cited in Clay and Leong (1974).

Morse, P.M. and J. Ingard (1968). *Theoretical Acoustics* (McGraw-Hill, New York), pp. 259-270, 441-449.

Urick, R.J. (1967). *Principles of Underwater Sound for Engineers* (McGraw-Hill, New York), p. 225.

5. SEISMIC PROFILING AT 3.5 kHz

5.1 Background Discussion

In Sec. 5, we will consider measurements of sub-bottom structure using the Modular Acoustic System on ALVIN, operating at 3.5 kHz.

Studies of the sedimentary and rock structures underlying the sea floor have relied heavily on the general set of techniques known as seismic profiling (Hill, 1963; Maxwell, 1970). These techniques include not only measurements with sources such as sparkers and air guns, which concentrate their energy at frequencies 100 Hz and below, but also with echo-sounding transducers operating at 3.5 kHz. The criteria for choice of these systems have included depth of penetration below the sea floor (for which the low-frequency systems are used) and fineness of resolution in observed structure (which have more often relied on the higher frequency system). Concern about resolution has resulted in the operation of 12-kHz systems just above the sea floor with very short pulse lengths of about 0.2 msec (Dow, 1964, 1975).

The correlation of acoustic horizons with layering in cores taken in the same region is a common goal of geophysical investigators. There have been some instances of striking success, such as in the Tyrrhenian Basin (Ryan *et al.*, 1965; Hastrup, 1970) where there is widespread horizontal homogeneity in the sediments. However, other effects have been frustratingly unsuccessful. Knott (1975) has mentioned the nearly total lack of success in relating seismic profiling measurements at 3.5 kHz with the core samples taken in the Giant Piston Corer (Hollister *et al.*, 1973; Silva and Hollister, 1973). The transducer which Knott has

employed has a 3-dB beamwidth of 30° and is hull-mounted on surface ships. In typical operating depths of 1000 to 5000 m, this insonifies large areas of the ocean floor. Except in those rare instances where the sea floor and the underlying sedimentary and rock horizons are totally smooth, there will be significant energy returns, as a result of scattering processes, at many angles of incidence other than the angle for specular reflection (Clay and Leong, 1974). Thus, any one pulse in the acoustic measurement samples a wide area which often has variable characteristics, such as the depth of the horizon. Under these circumstances, it is indeed rare that the core, taken at one discrete point, would show the same fine structure as shown in the acoustic measurement.

Part of this same problem with measurements made from the surface is the pictorial distortion which occurs in the representations of the bottom and sub-bottom topography found on facsimile recorders. As the terrain roughens and slopes become steeper, there are "side echoes" added to the bottom echoes particularly when the reflector is more concave than the wavefront. With a single pass over an area, the proper topography cannot be recovered, although if multiple passes are made throughout the region the technique of "migration" may be applied to resolve many ambiguities (Grant and West, 1965).

All these problems arise because the illuminated area on the bottom is too large. The area, in turn, is determined by the depth and the beamwidth of the transducer. The obvious solutions are reducing the beamwidth in surface systems or placing the transducer much closer to the ocean floor. Narrower beamwidths have been implemented in Navy survey ships (Maley *et al.*, 1974), and the usefulness of placing the transducer closer

to the ocean floor has been dramatically displayed in Scripps' towed underwater vehicle, Deep Tow (Lonsdale *et al.*, 1974). Deep Tow shows penetration of up to 100 m into sediments at 4.0 kHz and eliminates many pictorial distortions with the same 4.0 kHz system.

Operating the Modular Acoustic System with a tuned transducer at 3.5 kHz should yield comparable improvements. When the submersible skims beneath the ocean surface just 10 m above the bottom, small areas will be illuminated, permitting more accurate comparison with cores and the construction of more accurate maps of both bottom and sub-bottom topography.

5.2 Penetration into the Bottom

Of immediate interest is the depth of penetration into the bottom which one might expect using the Modular Acoustic System. This has not been tested at sea. However, we can make an estimate through a comparison of the operating parameters of the Modular Acoustic System with those of two 3.5/4-kHz systems that have successfully penetrated bottom sediments. They are the Woods Hole Oceanographic Institution shipboard system (Knott, 1975) and the Scripps Institution of Oceanography system, Deep Tow (Lonsdale *et al.*, 1974; Spiess and Tyce, 1973). Table 5.1 summarizes important operating data supplied by the cited sources. The data for the Modular Acoustic System are found in McElroy (1975) and unpublished data. The purpose is to estimate a maximum penetration for the Modular Acoustic System at both 3.5 kHz and at an alternate higher frequency (6 kHz) with a narrower beamwidth.

We will employ the simplest possible model in making the comparison. Equation 5.1 is taken from Clay and Leong (1974,

TABLE 5.1 COMPARISON OF THREE 3.5/4-KHZ SYSTEMS AND ONE SYSTEM AT 6 KHZ FOR BOTTOM PENETRATION.

System	20 log P_s re 1 ubar at 1 m	Receiver Sensitivity re 1 V/ubar	Beamwidth	Water Depth Between Source and Bottom, R_s	Attenuation at Frequency of System (4.3K)	Best Penetration Observed, r
WHOI Shipboard at 3.5 KHz	116 dB	-50.4 dB	20°	1000 to 5000 m Use 2000 = R_s	0.15 dB/m	1/4 sec of two-way travel time = 175 m
Scripps Deep Tow at 4.0 KHz (estimated from acoustic power of 500 W)	105 dB	-69.0 dB	Omnidirectional in one plane, 70° in another	10 m	0.17 dB/m	100 m
Modular Acoustic System at 3.5 kHz	100 dB estimate	-84.0 dB	60°	10 m	0.15 dB/m	180 m - based on comparison with Deep Tow
Modular Acoustic System at 6 kHz	107 dB estimate	-77.0 dB	-12°	10 m	0.26 dB/m	190 m - based on comparison with WHOI shipboard
						75 m - based on comparison with Deep Tow
						130 m - based on comparison with WHOI shipboard

Eq. 1.1) and gives the ensemble average of the specularly reflected pressure at a receiver, $\langle p \rangle$, where the source level at 1 m is p_0 , and the source and receiver distances in the specular directions are R_1 and R_2 , respectively. $\langle V \rangle$ is the ensemble average of the reflectivity coefficient.

$$\langle p \rangle = \frac{p_0}{(R_1 + R_2)} \langle V \rangle . \quad (5.1)$$

This expresses loss caused by spherical spreading of the specularly reflected wave. For a common source and receiver, $R_1 = R_2 \equiv R$. We will ignore the changes in R caused by refractive effects in the bottom, but will include the losses due to attenuation in the sediment, α , by modifying Eq. 5.1 as follows:

$$\langle p \rangle^2 = \frac{p_0^2}{4R^2} \langle V \rangle^2 e^{-2\alpha r} . \quad (5.2)$$

R is the sum of two parts, R_0 and r ,

$$R = R_0 + r , \quad (5.3)$$

where R_0 is the water depth from source to the bottom, and r is the distance into the bottom to the reflecting surface characterized by reflectivity $\langle V \rangle$.

Thus, the model expressed by Eq. 5.2 is that the intensity at the receive hydrophone is determined (1) by the source level p_0 , (2) by spherical spreading of the wave from the source into the sediment down to the reflecting horizon with reflectivity $\langle V \rangle$ and back to the source, and (3) by the attenuation in the sediment over the distance r and back within the sediment.

We can compute $\langle p \rangle^2$ for the Modular Acoustic System and equate it to $\langle p \rangle^2$ for either of the two other systems, thereby determining an estimated value of r for the Modular Acoustic System. Equating the two expressions for $\langle p \rangle^2$ assumes that the signal-to-noise discrimination of the two systems are equivalent.* We also assume that the reflection coefficients $\langle v \rangle$ at the maximum depth of penetration of each of the systems are equal.

α is determined from Hamilton (1974), who shows a value of 0.15 dB/m at 3.5 kHz for clayey silt and silty clay, increasing to 2 dB/m for sands. Since we are making comparisons for maximum penetration, we use the 0.15 figure, so that, after converting to decibels,

$$4.34\alpha = 0.15 \text{ dB/m} . \quad (5.4)$$

Dividing Eq. 5.2 for $\langle p \rangle^2$ for the WHOI or Deep Tow system (we use superscript "WHOI" for either of these) by that for the Modular Acoustic System (superscript "sub") and taking logarithms, we get

$$10 \log \frac{(\langle p \rangle^2)^{\text{sub}}}{(\langle p \rangle^2)^{\text{WHOI}}} = 0 = 20 \log P_0^{\text{sub}} - 20 \log P_0^{\text{WHOI}} + 20 \log \frac{R_0^{\text{WHOI}} + r^{\text{WHOI}}}{10 + r^{\text{sub}}} + 2(4.34\alpha)^{\text{WHOI}} r^{\text{WHOI}} - 2(4.34\alpha)^{\text{sub}} r^{\text{sub}} . \quad (5.5)$$

*We have excluded the receive sensitivity of the transducers from this calculation. Receive sensitivity would be critically important to the determination of signal to noise, were it so low that the preamplifier noise level in the receive-system electronics set the noise floor. Actually, for all the systems listed in Table 5.1, the contribution of noise from state-of-the-art preamplifiers at the frequencies in question (3.5, 4.0, and 6.0 kHz) is less than sea-state-zero noise, that is, less than minimum noise levels external to the systems.

All quantities in this equation are given in Table 5.1 except r^{sub} . Solving for r^{sub} , using the WHOI-surface-system data, gives

$$r^{\text{sub}} = 190 \text{ m.} \quad (5.6)$$

That is, based on a comparison with the Woods Hole surface system, we might expect a penetration of about 190 m in low attenuation sediments with the Modular Acoustic System operating at 3.5 kHz.

A similar calculation can be carried out comparing the penetration of the WHOI system in low attenuation sediments (0.15 dB/m) and the Modular Acoustic System in high attenuation sediments (2 dB/m). The penetration predicted for the submersible system is $r^{\text{sub}} = 18.5 \text{ m.}$

Lower penetrations are predicted by comparison with the Deep Tow system than with the WHOI system, possibly as a result of the shorter pulse lengths Deep Tow uses (0.5 to 1 msec). In sediments with attenuation of 0.15 dB/m the predicted penetration is 98 m, while in sediments with attenuation of 2 dB/m the predicted penetration is 11 m.

Although attenuation in sediments expressed in dB/m increases in direct proportion to the frequency (Hamilton, 1974), the beamwidth of the Modular Acoustic System's transducer has decreased from 60° at 3.5 kHz to about 40° at 6.0 kHz. This decreased beamwidth may be an advantage in some situations where increased spatial resolution is necessary, provided the investigator is willing to accept decreased depth of penetration. The increased attenuation is slightly offset by an increase in source

level by 7 dB at 6.0 kHz compared to 3.5 kHz. The predicted penetration in low attenuation sediments at 6.0 kHz (0.26 dB/m), based on a comparison with the WHOI system, is 130 m.

On the basis of these comparisons, the Modular Acoustic System has more than adequate penetration to study sediments within the depth range of normal cores or even of the Giant Piston Core which can penetrate up to 30 m (Hollister *et al.*, 1974). The smaller areas of the bottom which it insonifies make possible fine-scale comparisons with these cores. Operations at frequencies other than 3.5 kHz, such as 6.0 kHz, may be appropriate; even higher frequencies could be selected, based on the penetration of the core, for with higher frequency there is reduced beamwidth and increased spatial resolution.

5.3 Supplemental Instrumentation

Supplemental instrumentation falls into two classes. The first is those components and systems necessary to carry out the seismic profiling in a meaningful way, and include the ALNAV navigation system (Hunt *et al.*, 1974), a precise depth indicator, and a time base analogous to the 60 cycles used in facsimile recorders. The second class is coring tools and other sampling devices for the bottom.

5.3.1 ALNAV

Generally, seismic profiling by ALVIN would be carried out in a small area which was to be studied in detail. Investigators would generally wish to return for such tasks as sampling, coring, and photography. Thus, it is essential to carry out the seismic profiling survey within a navigational network. That network is provided by the ALNAV system designed specifically for ALVIN, which positions ALVIN in three dimensions.

Use of the navigation network is not a simple matter. Care must be taken in setting the transponders that it employs properly relative to the area to be studied. Otherwise, navigation errors will be greatly increased. Since navigation is important to so many ALVIN operations, including many of an acoustic character, we reproduce here a summary of conversations held with William Marquet (1975) concerning navigational accuracy.

Overall, there is no simple answer to the accuracy question. It is dependent on a number of factors, including slant-range standard error, geometrical errors associated with the ship's position during transponder net survey, and position of the submersible relative to the base lines of the transponder net.

There is no single summary of errors. Rather, the total picture must be inferred from a variety of documents:

- Marquet (1973) shows the "jitter" or minimal error associated with trying to return to the same point after following an arbitrary course. That error is 1.5 to 2.0 m (see p. 15 of Marquet for a figure summary of this experiment).
- Marquet and Smith (1974) contains the summary of an error analysis of ALVIN's position, assuming certain errors in the net survey. This summary is taken from an unpublished report by James Metzler.
- Hunt *et al.* (1974) contains a mathematical analysis of errors by Smith, giving particular attention to transponder network design and surveying.

The navigational problem and its associated errors can be summarized as follows, after taking note that it divides into

two major parts, net survey and submersible position:

1. Three transponders are placed on the bottom in a nominal triangle. Six coordinates must be determined: depth for the first transponder, depth and x coordinate for the second, and depth plus x and y coordinates for the third. The final coordinate of interest - namely, the rotation of this network relative to north - has not been determined with any precision nor has there been an error analysis (Marquet thinks it might be within one-half of a degree).

2. The transponder positions are determined from slant ranges to them, taken from six ship positions. These slant ranges must be calculated from the actual travel times and hence require a good knowledge of the sound velocity profile. Making determination of slant ranges from more than six positions permits one to calculate the slant-range error. This is expressed as the slant-range standard error (one sigma). From 24 ship positions, with a 5000-m baseline in the net and a 5000-m depth, a sigma of 3.3 m was measured. On two other occasions, sigmas of 2.7 m and 0.4 m were determined.

3. The errors in the transponder network are, then, these slant-range standard errors multiplied by a factor as low as 1.5 and as high as 10 to 20. The multiplication factor is determined from geometry - namely, the position of the ship relative to the net in its six (or more) survey positions. Good and bad geometry are shown in Hunt *et al.* (1974). The first part of the problem is now complete; transponder network accuracy is given. Marquet (1975) gives a normal multiplicative factor of 2 for good geometry, 3 for slightly less good. These are presumably operationally attainable factors.

4. The slant-range standard error applies to the determination of submersible position as well as to the network survey. The errors are now added to give further errors in position. This error analysis is given in the table on page 16 of Marquet and Smith (1974), assuming certain errors in the survey and slant ranges (these varied from 1 m to 3 m). The submersible's position error on the baseline can be huge - 225 m at a transponder, rising to 350 m at a point midway between two transponders. Well within the network, these reduce to 8 to 15 m.

5. Note that these errors are absolute errors, i.e., absolute position relative to the network. However, these errors are not a "jitter" error. They are a fixed error unless the sound velocity profile should change significantly. Thus, relative positions will be known with far more precision. Referring again to Fig. 6 on page 16 of Marquet and Smith (1974), we consider a traverse from a y position of 4800 m, x = 2000 m to y = 4800, x = 2400. The absolute errors are 12 and 13 m, respectively, which means that the error in their relative positions is only 1 m.

6. This establishes the importance of operating well within the net to reduce both absolute and relative errors. The change in absolute error as ALVIN changes position implies that the pattern traced out will be distorted, the distortion increasing as range from the starting point increases.

7. The fact that these errors are nearly fixed and have relatively little "jitter" was shown by an experiment in which the submersible was repeatedly returned to the same spot on the ocean floor. Its position at any moment may have been poorly known in an absolute sense, but the unchanging character of these errors was shown by the ability to return within 1.5 to 2 m of the starting point.

In conclusion, an investigator must decide whether absolute or only relative positional accuracy is important. In either case, minimum errors occur when the navigational network is properly surveyed, and ALVIN operates well within the network.

5.3.2 Precision depth indicator

ALVIN's motion up and down in the water column as it makes a traverse introduces error into the seismic recording. Wiggles in the bottom shown on ALVIN's display or a facsimile recorder could be caused either by actual microtopography or by fluctuations in ALVIN's depth. Precise depth measurements would eliminate this error. Actually, all that is needed is an indication of relative change in depth, since the absolute value is unimportant in making the correction.

This depth variation can be used to correct the seismic profile record after the dive. A more elegant solution is found in Spiess and Tyce (1973), where depth variation is used to delay the keying time of the Deep Tow transmitter.

A detailed consideration of instrumentation for this purpose is found in Sec. 4.5.

5.3.3 Precision time base

In shipboard seismic profiling, the time base is determined by the facsimile recorder on which the acoustic returns from sedimentary layers are displayed. When seismic data are taken in ALVIN and tape recorded, investigators will want to play back those recordings under a variety of filter conditions and sweep speeds so as to generate the optimum facsimile recorder

display. If this is to be accomplished, a 60-cycle time base, tied to the pulse repetition rate, must be implemented in the Modular Acoustic System and that 60-cycle time base must be recorded during any profiling.

5.3.4 Cores

Deep Cores. Deep coring will still need to be controlled from the surface. However, the navigation network which determined ALVIN's path in seismic profiling; an area can be used to guide a core from the surface to the desired site on the bottom. The ALNAV system has already performed such tasks with a large array and with devices such as cameras on long cables (Hunt *et al.*, 1974).

Shallow Cores. Small cores held by ALVIN's arm have been designed and built (Winget and McCamis, 1967; Winget, 1969) but their penetration is slight. The rock drill designed under the ARPA contract can take a core 2 m long, but cannot be used in sediments since it clogs (von Herzen and Williams, 1972). A further problem with the rock drill is its great weight (Wilson, 1975). It cannot be deployed from ALVIN until completion of the large ancillary platform known as SCAMP, which will have the strength to support the drill.

5.4 Conclusions

The Modular Acoustic System operated at 3.5 kHz should have excellent penetration in seismic profiling studies. At higher frequencies, the System should still provide sufficient penetration for comparison of acoustically determined horizons with

those shown by cores; operation at the higher frequencies will, in addition, provide even better spatial resolution than at 3.5 kHz because of the smaller beamwidth.

Seismic profiling experiments from ALVIN will require (1) use of the navigational information provided by ALNAV, (2) a precise record of depth changes, and (3) a 60-cycle reference signal.

Coring is a natural adjunct to the collection of seismic data by ALVIN. Both can be restricted to small areas on the ocean bottom to better the chances of meaningful correlation of the two measurements.

REFERENCES, SEC. 5

Clay, C.S. and W.K. Leong (1974). "Acoustic Estimates of the Topography and Roughness Spectrum of the Sea Floor Southwest of Iberian Peninsula," in *Physics of Sound in Marine Sediments*, L. Hampton, Ed. (Plenum Press, New York), pp. 373-380.

Dow, W. (1964). "Deep-Towed Echo Ranging Vehicle," *J. Underwater Acoustics* 14:289-299.

Dow, W. (1975). Woods Hole Oceanographic Institution. Personal communication.

Grant, F.S. and G.F. West (1965). *Interpretation Theory in Applied Geophysics* (McGraw-Hill, New York), pp. 156-161.

Hamilton, E.L. (1974). "Geoacoustic Models of the Sea Floor," in *Physics of Sound in Marine Sediments*, L. Hampton, Ed. (Plenum Press, New York), Fig. 1 on p. 196.

Hastrup, O.F. (1970). "Digital Analysis of Acoustic Reflectivity in the Tyrrhenian Abyssal Plain," *J. Acoust. Soc. Am.* 47: 181-190.

Hill, M.N., Ed. (1963). *The Sea, Vol. 3, The Earth Beneath the Sea* (Interscience, New York), especially the four articles: Ewing, J., "Elementary Theory of Seismic Refraction and Reflection Measurements, pp. 3-19; Shor, G.G., "Refraction and Reflection Techniques and Procedures," pp. 20-38; Hill, M.N., "Single-Ship Seismic Refraction Shooting," pp. 39-46; Hersey, J.B., "Continuous Reflection Profiling," pp. 47-72.

Hollister, C.D., A.J. Silva, and A. Driscoll (1973). "A Giant Piston-Corer," *Ocean Engineering* 2:159-168.

Hollister, C.D., A.J. Silva, and A. Driscoll (1974). "A New Giant Piston Core," in *Summary of Investigations Conducted in 1973, WHOI-74-18* (Woods Hole Oceanographic Institution, Woods Hole, Mass.), pp. GG-56,57.

Hunt, M.M., W.M. Marquet, D.A. Moller, K.R. Peal, W.K. Smith, and R.C. Spindel (1974). "An Acoustic Navigation System," Technical Report WHOI-74-6 (Woods Hole Oceanographic Institution, Woods Hole, Mass.).

Knott, S.T. (1975). Woods Hole Oceanographic Institution. Personal communication.

Lonsdale, P.F., R.C. Tyce, and F.N. Spiess (1974). "Near-Bottom Acoustic Observations of Abyssal Topography and Reflectivity," in *Physics of Sound in Marine Sediments*, L. Hampton, Ed. (Plenum Press, New York), pp. 293-317.

Maley, T.S., F.D. Sieber, and G.I. Johnson (1974). "Topography and Structure of the Western Puerto Rico Trench," *Geol. Soc. Am. Bull.* 85:513-518.

Marquet, W.M. (1973). "Submerged Navigation and Submersible Instrumentation," in *Technical Progress Report, Advanced Marine Technology, 1 Feb. 72 - 31 July 72, WHOI-73-20*, A.E. Maxwell (Woods Hole Oceanographic Institution, Woods Hole, Mass.) pp. 3-19.

Marquet, W.M. and W.K. Smith (1974). "Submerged Navigation," in *Technical Progress Report, Advanced Marine Technology, 1 Aug. 73 - 31 Jan 74, WHOI-74-27*, E.E. Hays (Woods Hole Oceanographic Institution, Woods Hole, Mass.), pp. 1-23.

Marquet, W.M. (1975). Woods Hole Oceanographic Institution. Personal communication.

Maxwell, A.E., Ed. (1970). *The Sea, Vol. 4, New Concepts of Sea Floor Evolution, Part I* (Wiley Interscience, New York), especially two articles: Ewing, J. and M. Ewing, "Seismic Reflection," pp. 1-51; Ludwig, W.J., J.E. Nafe, and C.L. Drake, "Seismic Refraction," pp. 53-84.

McElroy, P.T. (1975). "Design Features of the Submersible Modular Acoustic System," BBN Report No. 3060 (Bolt Beranek and Newman Inc., Cambridge, Mass.), 42 pp.

Ryan, W.B.F., F. Workman, and J.B. Hersey (1965). "Sediments on the Tyrrhenian Abyssal Plain," *Geol. Soc. Am. Bull.* 76:1261-1282.

Silva, A.J. and C.D. Hollister (1973). "Geotechnical Properties of Ocean Sediments Recovered with Giant Piston Corer," *J. Geophys. Res.* 78:3597-3616.

Spiess, F.N. and R.C. Tyce (1973). "Marine Physical Laboratory Deep Tow Instrumentation System," Scripps Institution of Oceanography Reference No. 73-4 (University of California, San Diego, California).

von Herzen, R.P. and D.L. Williams (1972). "A Self-Contained Deep Sea Rock Drill," in *Technical Progress Report, Advanced Marine Technology, 1 Aug 71 - 31 Jan 72, WHOI-72-90*, A.E. Maxwell (Woods Hole Oceanographic Institution, Woods Hole, Mass.), pp. 31-44.

Wilson, V. (1975). Woods Hole Oceanographic Institution. Personal communication.

Winget, C.L. and M.J. McCamis (1967). "A Technical Guide to the Deep Submergence Research Vehicle (DSRV) ALVIN for Use in Planning Scientific Missions," Technical Report 67-67 (Woods Hole Oceanographic Institution, Woods Hole, Mass.), Fig. 20.

Winget, C.L. (1969). "Hand Tools and Mechanical Accessories for a Deep Submersible," Technical Report 69-32 (Woods Hole Oceanographic Institution, Woods Hole, Mass.).